Received: 9 November 2023 | Revised: 16 January 2024 | Accepted: 30 January 2024

DOI: 10.1111/sapm.12675

STUDIES IN APPLIED MATHEMATICS WILEY

ORIGINAL ARTICLE

Bifurcations and global dynamics of a predator–prey mite model of Leslie type

Yue Yang[1,2] | **Yancong Xu**[1] | **Libin Rong**[3] | **Shigui Ruan**[4]

[1]Department of Mathematics, China Jiliang University, Hangzhou, China

[2]School of Mathematical Sciences, Qufu Normal University, Qufu, China

[3]Department of Mathematics, University of Florida, Gainesville, Florida, USA

[4]Department of Mathematics, University of Miami, Coral Gables, Florida, USA

Correspondence
Yancong Xu, Department of Mathematics, China Jiliang University, Hangzhou 310018, China.
Email: Yancongx@cjlu.edu.cn

Funding information
National Science Foundation, Grant/Award Numbers: 2324692, 1950254

Abstract

In this paper, we study a predator–prey mite model of Leslie type with generalized Holling IV functional response. The model is shown to have very rich bifurcation dynamics, including subcritical and supercritical Hopf bifurcations, degenerate Hopf bifurcation, focus-type and cusp-type degenerate Bogdanov–Takens bifurcations of codimension 3, originating from a nilpotent focus or cusp of codimension 3 that acts as the organizing center for the bifurcation set. Coexistence of multiple steady states, multiple limit cycles, and homoclinic cycles is also found. Interestingly, the coexistence of two limit cycles is guaranteed by investigating generalized Hopf bifurcation and degenerate homoclinic bifurcation, and we also find that two generalized Hopf bifurcation points are connected by a saddle-node bifurcation curve of limit cycles, which indicates the existence of global regime for two limit cycles. Our work extends some results in the literature.

KEYWORDS

Bogdanov–Takens bifurcation, cusp of codimensions 2 and 3, focus of codimension 3, Hopf bifurcation, predator–prey system, saddle-node bifurcation of limit cycles

MSC CLASSIFICATION

37G05, 37G10, 37G15, 37N25

1 | INTRODUCTION

To mitigate the loss of crops and fruits, many pest control measures have been exploited.[1–9] Chemical or biological measures are widely used in the control of pests. Pesticides are usually effective in killing pests but they can induce pest resistance, pest resurgence, and pesticide residues as mentioned by Schmidt.[9] Biological control has received more attention in recent years.[2,8] Based on a geographic analysis including North America, Europe, and Asia-Pacific, it is reported that the global biological pest control market is expected to be around 29 billion US dollars by 2025 with a compound annual growth rate of 5.7% in the given forecasting period.[10] The biological control has additional advantages in stopping the development of miticide resistance. Once established, it is also sustainable and can provide long-term control.

The predaceous mite, *Metaseiulus occidentalis* Nesbitt, is a generalist predator found in North America, Asia, and Oceania. Its prey, the McDaniel spider mite, *Tetranychus mcdameii* McGregor mainly found in North America, can reduce the apple or pear production, causing significant yield loss. This type of mites is the predominant mite pest species of Washington apples. Miticides were often used to kill them. However, some insecticides, including Carbamate and pyrethroid insecticides, are also highly toxic to mite predators, and thus should be avoided if possible. The conservation of predator mites in apple orchards is critical to the control of these mites.[3–5,9] A further investigation of the biological control using mite predators would provide great benefit to the increase of fruit production while decreasing the use of pesticides.

Studying the interactions between predators and their prey is one of the crucial research areas in ecology. Many mathematical models have been developed, analyzed, and compared with field data. Based on the model presented by May,[11] Wollkind et al.[1,12] proposed a predator–prey model describing mite interactions in fruit trees in Washington State of the following form:

$$\begin{cases} \frac{dx}{dt} = rx(1-\frac{x}{K}) - yp(x), \\ \frac{dy}{dt} = sy\left(1-\frac{y}{hx}\right), \end{cases} \tag{1}$$

where $x(t)$ and $y(t)$ represent the densities of prey and predators at time t, respectively. Their growth is assumed to obey the logistic rule, r and s are their respective intrinsic growth rates, while the carrying capacities of the two are K and hx, respectively, where h is a measure of the quality of prey for the predators, which is referred to as the Leslie function proposed by Leslie.[13]

The function $p(x)$ describes the update of the prey by predators. It may depend on many factors, such as the prey density, the physical state of the predators, and environmental conditions. Hence, various types of functional response have been used.

(I) Lotka–Volterra type (Holling Type I) function:

$$p(x) = \frac{m}{2a}x, \quad x \le 2a; \quad p(x) = m, \quad x > 2a. \tag{2}$$

This is the simplest functional response and $m > 0$ is a constant representing the maximal growth rate of species. The parameter $a > 0$ is the half-saturation constant, that is, the density of prey at which the per capita predation rate is half of its maximum m. System (1) with Holling Type I function $p(x)$ given by (2) is referred to as the Leslie–Grower predator–prey model and its global stability has been studied in Refs. [14, 15].

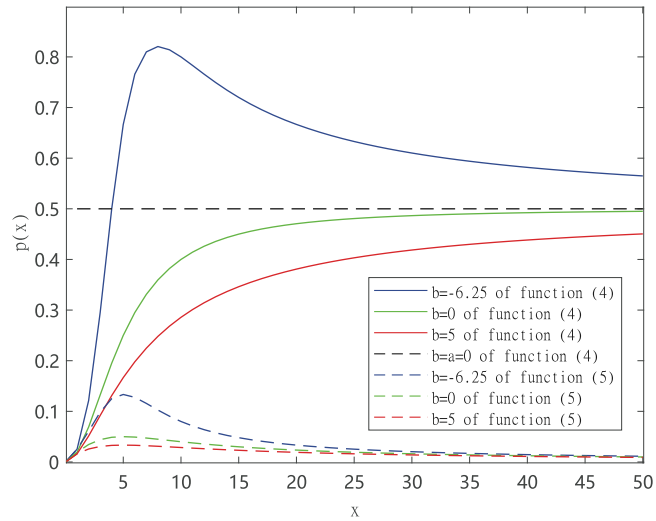

FIGURE 1 A comparison diagram of generalized Holling Type III function (4) and generalized Holling Type IV function (5). Here we assume $m = 0.5, a = 25$ as $b = -6.25, 0, 5$, respectively.

(II) Michaelis–Menten (Holling Type II) function:

$$p(x) = \frac{mx}{x + a}. \tag{3}$$

Here, $m > 0$ is a constant standing for the maximal growth rate of species and $a > 0$ is the half-saturation constant. System (1) with Holling Type II function $p(x)$ given by (3) is referred to as the Holling–Tanner predator–prey model and has been extensively studied in the literature, see Refs. [16–20]. For example, Sáez and González[18] described the bifurcation diagram of limit cycles that appear in the first realistic quadrant of the predator–prey model, and gave a qualitative description of the bifurcation curve when two limit cycles collapse on a semistable limit cycle and disappear.

(III) Sigmoidal (generalized Holling Type III) function:

$$p(x) = \frac{mx^2}{x^2 + bx + a}. \tag{4}$$

Here, $m, a > 0$ are positive constants and a is the half-saturation constant. The parameter $b > -2\sqrt{a}$ and the situation of $b = 0$ is the Holling Type III response function.[21,22] The difference between $b \geq 0$ and $b < 0$ of function (4) can be seen from Figure 1. This shows that when the number of prey is below a certain threshold, predators no longer obtain food by hunting prey because of learning behavior; when the number of prey is above this threshold, predators continue hunting prey until a saturation level is reached when $b \geq 0$. When $b < 0$, the predation increases to reach a peak, followed by a decline approaching m as x increases. Hence, $p(x)$ describes the circumstance where the prey can better protect themselves when their density is high enough. Predator–prey system of Leslie type with generalized Holling Type III functional response has been analyzed by many authors, see, for example, Refs. [14, 23–26]. Hsu and Huang[14] studied the global stability of equilibria and the existence of limit cycles.

(IV) Monod–Haldane (generalized Holling Type IV) function:

$$p(x) = \frac{mx}{x^2 + bx + a}. \tag{5}$$

Here, $m, a > 0$ are constants and $b > -2\sqrt{a}$. This function can be used to describe the effect of "inhibition" in microbial dynamics and "group defense" in population dynamics,[22,27,28] proposed by Andrews.[29] A comparison of the generalized Holling Type III function and generalized Holling Type IV function is shown in Figure 1. With the Type IV function, it can be shown that the prey can better protect themselves when their density is sufficiently high. See more applications of the Type IV functional response.[30–32]

When $b = 0$, the function $p(x) = \frac{mx}{x^2+a}$ is referred to as the Holling Type IV functional response. System (1) with Holling Type IV has been extensively investigated.[33–37] For example, Li and Xiao[33] showed that the model undergoes the codimension 2 Bogdanov–Takens bifurcation and the subcritical Hopf bifurcation in two small neighborhoods of the two nonhyperbolic positive equilibria, respectively. However, the parameter region of two-limit-cycle is not given. Huang et al.[35] studied the degenerate focus type Bogdanov–Takens bifurcation of codimension 3. Note that they did not consider degenerate cusp type Bogdanov–Takens bifurcation of codimension 3 and did not present the global bifurcation diagram in detail. Dai and Zhao[36] analyzed Hopf cyclicity and global dynamics for a predator–prey system of Leslie type with simplified Holling Type IV functional response. Ruan and Xiao[22] used the functional response with $b = 0$ to study the global bifurcation of a predator–prey system and showed the existence of codimension 2 Bagdanov–Takens bifurcation and a focus of multiplicity at least 2. Xiao and Zhu[38] studied a Gauss-type predator–prey system with a Holling IV functional response, yielding the Hopf bifurcation with codimension 2 and the existence of two limit cycles. Rothe and Shafer[39] studied a generalized Gauss type for the interaction of two species with the function (5) and obtained a codimension 2 cusp singularity. However, the global bifurcation diagram and transitions of bifurcation are not shown explicitly. It is worth describing the whole global bifurcation diagram and identifying the transitions among those different bifurcation regimes in details.

There are very few studies on system (1) with the generalized Holling Type IV function.[28,30] A model with temperature-dependent parameters for the mite interaction in apple trees was analyzed to determine how the type of functional response influences the bifurcation and stability behavior in Collings.[28] Recently, Atabaigi and Barati[30] presented a geometric analysis of relaxation oscillations and canard cycles in a singularly perturbed predator–prey system of Holling and Leslie types under the assumption $r \ll s$. However, the global bifurcation analysis of system (1) with generalized Holling Type IV is still not complete.

In this paper, we focus on the local and global dynamics of the predator–prey mite system of Leslie type (1) with generalized Holling IV functional response (5), given by

$$\begin{cases} \frac{dx}{dt} = rx(1 - \frac{x}{K}) - \frac{mxy}{x^2+cx+b}, \\ \frac{dy}{dt} = sy(1 - \frac{y}{hx}), \end{cases} \tag{6}$$

where $x > 0, y \geq 0, r, K, m, s$, and h are all positive parameters, $b > 0$ is the half-saturation constant, and $c > -2\sqrt{b}$ has the same explanation as before. For simplicity, we rescale x, y, t and

parameters in (6) by letting

$$\overline{x} = \frac{x}{K}, \overline{y} = \frac{my}{rK^2}, \overline{t} = rt, a = \frac{b}{K^2}, d = \frac{c}{K}, \delta = \frac{s}{r}, \beta = \frac{sK}{hm}.$$

Dropping the bars, we have the following reduced system:

$$\begin{cases} \frac{dx}{dt} = x(1-x) - \frac{xy}{x^2+dx+a}, \\ \frac{dy}{dt} = y(\delta - \frac{\beta y}{x}), \end{cases} \tag{7}$$

where a, δ, β are positive and $d > -2\sqrt{a}$. In this paper, we will study the global bifurcation dynamics and the details of transition among different parameter regimes. In particular, the role of "group defense" will be further revealed.

This paper is organized as follows. In the next section, we investigate the existence and type of equilibria of system (7). Section 3 is devoted to the bifurcation analysis including degenerate cusp-type Bogdanov–Takens bifurcation of codimensions 2 and 3, degenerate focus-type Bogdanov–Takens bifurcation of codimension 3, and Hopf bifurcation with codimension 2. In Section 4, numerical simulations including the global bifurcation diagrams and phase portraits are given. The paper ends with conclusion and discussion in Section 5.

2 | THE EQUILIBRIA OF SYSTEM (7)

From the biological feasibility, we restrict system (7) in $\mathbb{R}^+_2 = \{(x, y) : x > 0, y \geq 0\}$. By a straightforward analysis, we know that system (7) has only one boundary equilibrium $E_0(1, 0)$, which is a hyperbolic saddle indicating that the prey population reaches its carrying capacity in the absence of predators. Further, we have the following result.

Theorem 1. *The positive invariant and boundedness region of system (7) is the rectangular region* $\Omega = \{(x, y)|0 < x < 1, 0 \leq y \leq \frac{\delta}{\beta}\}$.

Proof. By the first equation of system (7), we have $\frac{dx}{dt}|_{x\geq 1} < 0$. Thus, we only focus on $0 < x < 1$. On the other hand, we can easily get $\frac{dy}{dt} = y(\delta - \frac{\beta y}{x}) < y(\delta - \beta y)$ for $0 < x < 1$, which leads to $\frac{dy}{dt}|_{y>\frac{\delta}{\beta}} < 0$. Therefore, all solutions of system (7) will ultimately move toward the region $\Omega = \{(x, y)|0 < x < 1, 0 \leq y \leq \frac{\delta}{\beta}\}$ and this ends the proof. □

Based on the above analysis, it is sufficient to discuss positive equilibria of system (7) in the rectangular region Ω. To do this, let

$$x(1-x) - \frac{xy}{x^2+dx+a} = 0, \quad y\left(\delta - \frac{\beta y}{x}\right) = 0,$$

which yields that

$$x^3 - (1-d)x^2 + (a + \frac{\delta}{\beta} - d)x - a = 0. \tag{8}$$

Assuming that x_1, x_2, x_3 are the three roots of (8) and $x_1 < x_2 < x_3$, then based on Vieta Theorem, we have

$$x_1 + x_2 + x_3 = 1 - d,\ \ x_1x_2 + x_1x_3 + x_2x_3 = a + \frac{\delta}{\beta} - d,\ \ x_1x_2x_3 = a. \tag{9}$$

In view of $a > 0$, Equation (8) has at least one and at most three positive roots; that is, system (7) has at least one and at most three positive equilibria $E_i(x_i, \frac{\delta}{\beta}x_i), i = 1, 2, 3$. Let

$$f(x) = x^3 + a_2x^2 + a_1x + a_0,$$

where $a_2 = d - 1, a_1 = a + \frac{\delta}{\beta} - d, a_0 = -a$.

To investigate the existence of positive equilibria $E_i(x_i, \frac{\delta}{\beta}x_i)(i = 1, 2, 3)$ of system (7) in the rectangular region $\Omega = \{(x, y)|0 < x < 1, 0 \le y \le \frac{\delta}{\beta}\}$, we only need to focus on the existence of positive root $x_i(i = 1, 2, 3)$ of $f(x) = 0$ in the interval (0,1). It is evident that

$$f'(x) = 3x^2 + 2a_2x + a_1.$$

On the one hand, the Jacobian matrix at any positive equilibrium $E(x, \frac{\delta}{\beta}x)$ of system (7) is given by

$$J(E) = \begin{pmatrix} 1 - 2x - \frac{(1-x)(a-x^2)}{x^2+dx+a} & -\frac{x}{x^2+dx+a} \\ \frac{\delta^2}{\beta} & -\delta \end{pmatrix}.$$

Direct calculation shows that

$$\begin{aligned} \det(J(E)) &= \frac{\delta x}{x^2 + dx + a} f'(x), \\ \mathrm{tr}(J(E)) &= 1 - 2x - \delta - \frac{(1-x)(a-x^2)}{x^2 + dx + a}. \end{aligned} \tag{10}$$

From the first expression of (10), we know that the equilibrium is an elementary equilibrium, a hyperbolic saddle, or a degenerate equilibrium if $f'(x) > 0, < 0$ or $= 0$, respectively.

On the other hand, denote

$$\Delta = a_2^2 - 3a_1.$$

Then, $f'(x) = 0$ has no real root if $\Delta < 0$, has one real root of multiplicity 2 if $\Delta = 0$, which is denoted by $x^* = -\frac{a_2}{3} = \frac{1-d}{3}$, and has two real roots if $\Delta > 0$, which are marked as $\bar{x}_1$ and $\bar{x}_2$ as

follows:

$$\bar{x}_1 = \frac{-a_2 - \sqrt{\Delta}}{3},$$
$$\bar{x}_2 = \frac{-a_2 + \sqrt{\Delta}}{3}. \tag{11}$$

Therefore, we can investigate the existence of positive root of $f(x) = 0$ in the interval (0,1) with three scenarios: $\Delta < 0$, $\Delta = 0$, and $\Delta > 0$. Let $x_{i,i+1}$ be the coincidence point of x_i and $x_{i+1}(i = 1, 2, 3)$, then the corresponding degenerate equilibria of system (7) are expressed as $E_{i,i+1}(x_{i,i+1}, \frac{\delta}{\beta}x_{i,i+1})(i = 1, 2, 3)$.

Scenario 1: $\Delta < 0$.

On this occasion, $f'(x) = 0$ has no real root and $f'(x) > 0, x \in (0, 1)$, which shows that $f(x)$ is a strictly monotone increasing function in the interval (0,1). Note that $f(0) = a_0 < 0$ and $f(1) = \frac{\delta}{\beta} > 0$, thus $f(x) = 0$ has a unique positive root in the interval (0,1), denoted as x_1 (or x_3).

Scenario 2: $\Delta = 0$.

In this scenario, $f'(x) = 0$ has one real root of multiplicity 2, marked as $x^* = \frac{1-d}{3}$ and $f'(x) \geq 0, x \in (0, 1)$, which demonstrates that $f(x)$ is monotonically increasing in the interval (0,1). Notice again that $f(0) < 0, f(1) > 0$ and $f(x^*) = \frac{2a_2^3 - 9a_1a_2 + 27a_0}{27}$, then we have the following:

(S2A) if $f(x^*) \neq 0$, then $f(x) = 0$ has a unique positive root, denoted by x_1 (or x_3);
(S2B) if $f(x^*) = 0$, then $f(x) = 0$ has a unique positive root of multiplicity 3, denoted by $x^* = \frac{1-d}{3}$.

Scenario 3: $\Delta > 0$.

In this situation, $f'(x) = 0$ has two real roots, which are marked as $\bar{x}_1$ and $\bar{x}_2$. Obviously, $\bar{x}_1$ and $\bar{x}_2$ are the maximum and minimum value points of $f(x)$, respectively. By analyzing the positions of $\bar{x}_1$ and $\bar{x}_2$, we have the following:

(S3A) When $\bar{x}_1 \geq 1$ or $\bar{x}_2 \leq 0, f'(x) > 0, x \in (0, 1)$ and the distribution of positive roots of $f(x) = 0$ in the interval (0,1) is the same as Scenario 1.
(S3B) When $0 < \bar{x}_1 < 1 \leq \bar{x}_2$, $f'(x)$ first monotonically increases in $(0, \bar{x}_1)$ and then monotonically decreases in $(\bar{x}_1, 1)$. Again note that $f(0) < 0$ and $f(1) > 0$, evidently we get that $f(x) = 0$ has a unique root in the interval (0,1), which is denoted by x_1.
(S3C) When $0 < \bar{x}_1 < \bar{x}_2 < 1$, $f(x)$ first monotonically increases in $(0, \bar{x}_1)$, then monotonically decreases in $(\bar{x}_1, \bar{x}_2)$, and finally monotonically increases in $(\bar{x}_2, 1)$. Again noting that $f(0) < 0$ and $f(1) > 0$, then based on the signs of $f(\bar{x}_1)$ and $f(\bar{x}_2)$, we can get the distribution of positive root of $f(x) = 0$ in the interval (0,1) as follows:
  (I) If $f(\bar{x}_1) > 0$ and $f(\bar{x}_2) < 0$, then $f(x) = 0$ has three positive roots, denoted by $x_1 < x_2 < x_3$;
  (II) if $f(\bar{x}_1) > 0$ and $f(\bar{x}_2) = 0$, then $f(x) = 0$ has two positive roots, and one of them is a positive root of multiplicity 2, denoted by $x_1 < \bar{x}_2 = x_{2,3}$;
  (III) if $f(\bar{x}_1) > 0$ and $f(\bar{x}_2) > 0$, then $f(x) = 0$ has one positive root, denoted by x_1;
  (IV) if $f(\bar{x}_1) = 0$, then $f(x) = 0$ has two positive roots, and one of them is a positive root of multiplicity 2, denoted by $\bar{x}_1 = x_{1,2} < x_3$;
  (V) if $f(\bar{x}_1) < 0$, then $f(x) = 0$ has a unique positive root, denoted by x_3.

(S3D) When $\bar{x}_1 \le 0 < 1 \le \bar{x}_2$, $f'(x) < 0, x \in (0,1)$, that is, $f(x)$ monotonically decreases in the interval (0,1), which contradicts with $f(0) < 0$ and $f(1) > 0$.

(S3E) When $\bar{x}_1 \le 0 < \bar{x}_2 < 1$, $f(x)$ is strictly monotonically decreasing in the interval $(0, \bar{x}_2)$ and monotonically increases in $(\bar{x}_2, 1)$. Then $f(x) = 0$ has a unique root in the interval (0,1), marked as x_3.

From above analysis, we can get the existence of positive equilibria of system (7) as follows.

Theorem 2. *System (7) has*

(I) a unique positive equilibrium $E_1(x_1, \frac{\delta}{\beta}x_1)$ *(or* $E_3(x_3, \frac{\delta}{\beta}x_3)$*) if one of the following conditions are satisfied:*
- *(i)* $\Delta < 0$;
- *(ii)* $\Delta = 0, f(x^*) \neq 0$;
- *(iii)* $\Delta > 0, \bar{x}_1 \ge 1$ *or* $\bar{x}_2 \le 0$, *or* $0 < \bar{x}_1 < 1 \le \bar{x}_2$;
- *(iv)* $\Delta > 0, 0 < \bar{x}_1 < \bar{x}_2 < 1, f(\bar{x}_1) > 0$, *and* $f(\bar{x}_2) > 0$ *or* $f(\bar{x}_1) < 0$;
- *(v)* $\Delta > 0$ *and* $\bar{x}_1 \le 0 < \bar{x}_2 < 1$.

(II) A degenerate positive equilibrium $E^*(x^*, \frac{\delta}{\beta}x^*) = (\frac{1-d}{3}, \frac{(1-d)(d+2)^3}{81})$ *of multiplicity 3 if* $\Delta = 0$ *and* $f(x^*) = 0$.

(III) Two positive equilibria and one of them is a degenerate equilibrium if one of the following conditions is satisfied:
- *(i) an equilibrium* $E_1(x_1, \frac{\delta}{\beta}x_1)$ *and a degenerate equilibrium* $\bar{E}_2(\bar{x}_2, \frac{\delta}{\beta}\bar{x}_2)$, *where* $\bar{x}_2 = x_{2,3}$ *if* $\Delta > 0, 0 < \bar{x}_1 < \bar{x}_2 < 1$, *and* $f(\bar{x}_1) > 0$;
- *(ii) a degenerate equilibrium* $\bar{E}_1(\bar{x}_1, \frac{\delta}{\beta}\bar{x}_1)$ *and an equilibrium* $E_3(x_3, \frac{\delta}{\beta}x_3)$, *where* $\bar{x}_1 = x_{1,2}$ *if* $\Delta > 0, 0 < \bar{x}_1 < \bar{x}_2 < 1$, *and* $f(\bar{x}_1) = 0$.

For the sake of convenience, we denote degenerate equilibria $\bar{E}_1(\bar{x}_1, \frac{\delta}{\beta}\bar{x}_1)$ *(or* $\bar{E}_2(\bar{x}_2, \frac{\delta}{\beta}\bar{x}_2)$*) as* $E_*(x_*, \frac{\delta}{\beta}x_*)$.

(IV) Three positive equilibria $E_i(x_i, \frac{\delta}{\beta}x_i), i = 1,2,3$ *if* $\Delta > 0, 0 < \bar{x}_1 < \bar{x}_2 < 1, f(\bar{x}_1) > 0$, *and* $f(\bar{x}_2) < 0$.

Here, $\bar{x}_1$ *and* $\bar{x}_2$ *are defined as (11), respectively.*

Remark 1. When system (7) has three positive equilibria $E_i(x_i, \frac{\delta}{\beta}x_i), i = 1,2,3$, that is, when the condition (IV) in Theorem 2 is satisfied, then $f'(x_2) < 0$. In view of the first expression of (10), we obtain that E_2 is a saddle.

2.1 | Cusp of codimensions 2 and 3

In this subsection, we study the case (III) in Theorem 2 and explore conditions such that $E_1(x_1, \frac{\delta}{\beta}x_1)$ (or $E_3(x_3, \frac{\delta}{\beta}x_3)$) is a nonhyperbolic equilibrium with $\mathrm{tr}(J(E_1)) = 0$ and the degenerate equilibrium $E_*(x_*, \frac{\delta}{\beta}x_*)$ satisfies $\mathrm{tr}(J(E_*)) = 0$.

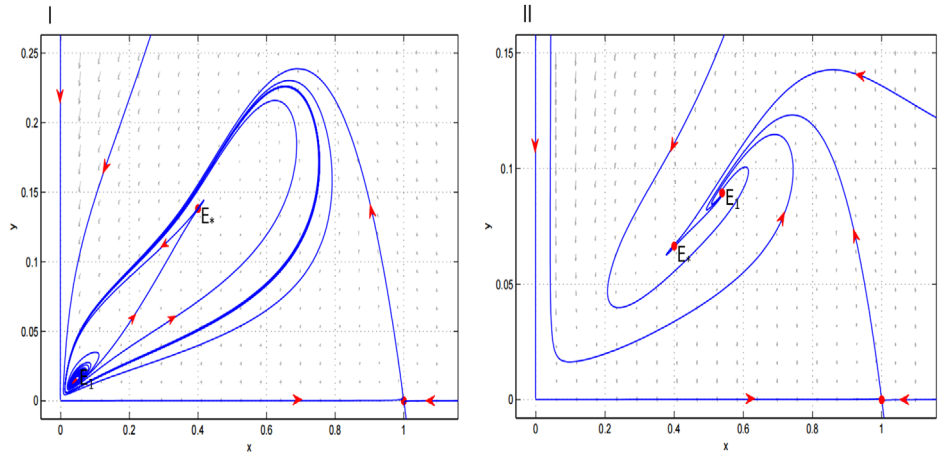

FIGURE 2 The phase portraits of Theorem 3. I: the coexistence of a stable weak focus with multiplicity 1, $E_1(\frac{1}{25}, \frac{216}{15625})$, and a cusp of codimension 2, $E_*(\frac{2}{5}, \frac{632}{3125})$, with $d = \frac{4}{25}, a = \frac{4}{625}, \delta = \frac{3}{5}, \beta = \frac{125}{72}$; II: the coexistence of a stable hyperbolic focus $E_1(\frac{7}{13}, \frac{378}{4225})$ and a cusp of codimension 3, $E_*(\frac{2}{5}, \frac{108}{1625})$, with $d = -\frac{22}{65}, a = \frac{28}{325}, \delta = \frac{3}{5}, \beta = \frac{65}{18}$.

Equations $f(x_*) = \det(J(E_*)) = 0$ and $\mathrm{tr}(J(E_*)) = 0$ lead to

$$a = x_*^2(1 - d - 2x_*), \quad \delta = 1 - x_*, \quad \beta = \frac{1}{(1 - x_*)(d + 2x_*)}, \tag{12}$$

where $0 < x_* < \min\{\frac{1-d}{2}, \frac{1}{2}\}(-2\sqrt{a} < d < 1)$ and $x_* \neq \frac{1-d}{3}$. Furthermore, $x_1 + 2x_* = 1 - d$, $\mathrm{tr}(J(E_1)) = 0$, and (12) result in

$$d = d_1 = x_*^2 - 5x_* + 2.$$

Actually, $d = 1 - 3x_*$ can also be generated in this way, while $d = 1 - 3x_*$ and $x_1 + 2x_* = 1 - d = 3x_*$ produce $x_1 = x_*$. That is, x_* is a triple root of $f(x) = 0$, which is a contradiction to case (ii). Hence $d \neq 1 - 3x_*$. On the other hand, letting $d_2 = \frac{2(x_*^2 - 4x_* + 1)}{3 - x_*}$, we have the following theorem.

Theorem 3. *Assume that the conditions (III) in Theorem 2 and (12) are satisfied, then system (7) has two different positive equilibria: $E_*(x_*, (1 - x_*)^2(d + 2x_*)x_*)$ and $E_1(x_1, \frac{\delta}{\beta}x_1)$ (or $E_3(x_3, \frac{\delta}{\beta}x_3)$) $= (1 - d - 2x_*, (1 - x_*^2)(d + 2x_*)(1 - d - 2x_*))$, where $0 < x_1 < x_* < x_3 < 1$. Furthermore,*

(I) when $d = d_1$,
  (i) E_1 (or E_3) is a stable weak focus with multiplicity 1;
  (ii) E_* is a cusp of codimension 2.
(II) When $d = d_2$,
  (i) E_1 (or E_3) is a stable hyperbolic focus (or node);
  (ii) E_* is a cusp of codimension 3.

The corresponding phase portraits are given in Figure 2.

Proof. We first concentrate on the proof of part (I) (i). Setting $dt = x(x^2 + dx + a)d\tau$ yields an equivalent system of (7) (we still denote τ by t)

$$\begin{cases} \frac{dx}{dt} = x^2(x^2 + dx + a)(1 - x) - x^2 y, \\ \frac{dy}{dt} = (x^2 + dx + a)y(\delta x - \beta y). \end{cases} \tag{13}$$

In view of $x(x^2 + dx + a) > 0$, the topological property of system (13) is the same as that of system (7). Next, let

$$\overline{x} = \frac{x}{x_1}, \ \overline{y} = \frac{y}{\frac{\delta x_1}{\beta}}, \ \tau = x_1 t. \tag{14}$$

Then we obtain a polynomial differential system equivalent to system (13) (we still denote τ by t)

$$\begin{cases} \frac{d\overline{x}}{dt} = x_1^3 \overline{x}^2 \left(\overline{x}^2 + \frac{d}{x_1}\overline{x} + \frac{a}{x_1^2} \right) \left(\frac{1}{x_1} - \overline{x} \right) - \frac{\delta x_1}{\beta} \overline{x}^2 \overline{y}, \\ \frac{d\overline{y}}{dt} = \delta x_1^2 \left(\overline{x}^2 + \frac{d}{x_1}\overline{x} + \frac{a}{x_1^2} \right) \overline{y}(\overline{x} - \overline{y}). \end{cases}$$

Setting

$$\overline{m} = \frac{1}{x_1}, \ \overline{d} = \frac{d}{x_1}, \ \overline{a} = \frac{a}{x_1^2}, \ \overline{\beta} = \frac{\delta x_1}{\beta}, \ \overline{\delta} = \delta x_1^2, \tag{15}$$

and removing the bars, we get the following system:

$$\begin{cases} \frac{dx}{dt} = \frac{1}{m^3} x^2(x^2 + dx + a)(m - x) - \beta x^2 y, \\ \frac{dy}{dt} = \delta y(x^2 + dx + a)(x - y). \end{cases} \tag{16}$$

$\overline{E}(1, 1)$ is an equilibrium of system (16) (corresponding to the equilibrium $E_1(x_1, \frac{\delta x_1}{\beta})$ in system (7)). We have

$$\beta = \frac{(1 + d + a)(m - 1)}{m^3}.$$

Substituting it into (16) generates the following system:

$$\begin{cases} \frac{dx}{dt} = \frac{1}{m^3} x^2(x^2 + dx + a)(m - x) + \frac{(1+d+a)(1-m)}{m^3} x^2 y, \\ \frac{dy}{dt} = \delta y(x^2 + dx + a)(x - y), \end{cases} \tag{17}$$

in which $a, m, \delta > 0$ and $d > -2\sqrt{a}$. As $d = d_1$ in the original system (7), we get $x_1 = -(x_*^2 - 3x_* + 1)$. By the conditions in (12), we know that $d = -\frac{x_*^2-5x_*+2}{x_*^2-3x_*+1}$, $a = -\frac{x_*^2}{x_*^2-3x_*+1}$, $m = -\frac{1}{x_*^2-3x_*+1}$, and $\delta = (1 - x_*)(x_*^2 - 3x_* + 1)^2$ in system (17).

Now we show that E_1 of system (7) (i.e., $\widetilde{E}(1, 1)$ of system (17)) is a stable weak focus with multiplicity 1. Setting $X = x - 1, Y = y - 1$ and substituting above d, a, m, and δ into system (17) result in a new system as follows (for convenience, in every subsequent transformation, we rename X, Y, τ as x, y, t, respectively):

$$\begin{cases} \frac{dx}{dt} = (x_*^2 - 3x_* + 1)\{-(1 - x_*)^3x + (2 - x_*)(1 - x_*)^3y - 2(2 - x_*) \\ \qquad \times (1 - x_*)^2x_*x^2 + 2(2 - x_*)(1 - x_*)^3xy + (5x_*^4 - 25x_*^3 + 40x_*^2 \\ \qquad - 23x_* + 4)x^3 + (2 - x_*)(1 - x_*)^3x^2y\} + o(|x, y|^3), \\ \frac{dy}{dt} = (x_*^2 - 3x_* + 1)\{-(1 - x_*)^3x + (1 - x_*)^3y - (1 - x_*)^2x_*x^2 \\ \qquad - (1 - x_*)^2(1 - 2x_*)xy + (1 - x_*)^3y^2 + (1 - x_*)(x_*^2 - 3x_* + 1)x^3 \\ \qquad - (1 - 2x_*)(1 - x_*)x^2y + (1 - x_*)^2x_*xy^2\} + o(|x, y|^3). \end{cases} \tag{18}$$

Taking $\nu = (1 - x_*)^{\frac{7}{2}}(x_*^2 - 3x_* + 1)$ and making the following scalings, $x = -(2 - x_*)(1 - x_*)^3(x_*^2 - 3x_* + 1)X$, $y = -(1 - x_*)^3(x_*^2 - 3x_* + 1)X - \nu Y$, $dt = \frac{1}{\nu}d\tau$, system (18) becomes

$$\begin{cases} \frac{dx}{dt} = y + f(x, y), \\ \frac{dy}{dt} = -x + g(x, y), \end{cases}$$

where

$$\begin{aligned} f(x, y) = {} & -2(2 - x_*)(1 - x_*)^{\frac{3}{2}}(x_*^2 - 3x_* + 1)^2x^2 - 2(2 - x_*)(1 - x_*)^3 \\ & \times (x_*^2 - 3x_* + 1)xy + (2 - x_*)^2(1 - x_*)^{\frac{5}{2}}(x_*^2 - 3x_* + 1)^3 \\ & \times (5x_*^2 - 11x_* + 5)x^3 + (2 - x_*)^2(1 - x_*)^6(x_*^2 - 3x_* + 1)^2x^2y \\ & + o(|x, y|^3), \\ g(x, y) = {} & -(1 - x_*)(x_*^2 - 3x_* + 1)(x_*^3 - 8x_*^2 + 14x_* - 5)x^2 + (1 - x_*)^{\frac{3}{2}} \\ & \times (x_*^2 - 3x_* + 1)(4x_*^2 - 9x_* + 4)xy + (2 - x_*)(1 - x_*)^2 \\ & \times (x_*^2 - 3x_* + 1)^2(4x_*^5 - 28x_*^4 + 74x_*^3 - 88x_*^2 + 45x_* - 8)x^3 \\ & - (1 - x_*)^3(x_*^2 - 3x_* + 1)y^2 + (2 - x_*)(1 - x_*)^{\frac{7}{2}}(x_*^2 - 3x_* + 1)^2 \\ & \times (x_*^3 - 8x_*^2 + 12x_* - 4)x^2y + x_*(2 - x_*)(1 - x_*)^5(x_*^2 - 3x_* + 1)^2xy^2 \\ & + o(|x, y|^3). \end{aligned}$$

Applying the formula in Perko,[40] we get the first Lyapunov coefficient as follows:

$$\begin{aligned}\sigma_1 &= \Big\{\frac{1}{16}(f_{xxx}+f_{xyy}+g_{xxy}+g_{yyy})-\frac{1}{16}(f_{xy}(f_{xx}+f_{yy})-g_{xy}(g_{xx}+g_{yy})\\ &\quad -f_{xx}g_{xx}+f_{yy}g_{yy})\Big\}\Big|_{x=y=0}\\ &= \frac{1}{8}(2-x_*)^2(1-x_*)^{\frac{5}{2}}(x_*^2-3x_*+1)^2(7x_*^4-25x_*^3+27x_*^2-15x_*+3).\end{aligned}$$

Because $0<x_*<\min\{\frac{1}{2},\frac{1-d}{2}\}(x_*\neq\frac{1-d}{3})$, we can assert that $\frac{3-\sqrt{5}}{2}<x_*<\frac{1}{2}$ when $d=d_1$. Then, we obtain $\sigma_1<0$. This completes the proof of (I) (i).

Next we verity the part (I) (ii) that the equilibrium E_* of system (7) is a cusp of codimension 2 when $d=d_1$. We translate E_* to the origin by the transformation $X=x-x_*, Y=y-(1-x_*)^2(d+2x_*)x_*$ and write the generated system in Taylor expressions as follows (for convenience, in every subsequent transformation, we rename X,Y as x,y, respectively).

$$\begin{cases}\frac{dx}{dt} = (1-x_*)x-\frac{1}{(1-x_*)(d+2x_*)}y+\left(\frac{1}{d+2x_*}-\frac{1}{1-x_*}-1\right)x^2+\frac{1}{(1-x_*)^2(d+2x_*)}xy\\ \qquad +o(|x,y|^2),\\ \frac{dy}{dt} = (1-x_*)^3(d+2x_*)x-(1-x_*)y-\frac{(1-x_*)^3(d+2x_*)}{x_*}x^2+\frac{2(1-x_*)}{x_*}xy\\ \qquad -\frac{1}{(1-x_*)(d+2x_*)x_*}y^2+o(|x,y|^2),\end{cases}$$

where a,δ,β have been substituted by the conditions in (12). Making the following scalings of coordinates

$$X=x,\ \ Y=(1-x_*)x-\frac{1}{(1-x_*)(d+2x_*)}y,$$

we obtain

$$\begin{cases}\frac{dx}{dt} = y+\left(-\frac{1}{1-x_*}+\frac{1}{d+2x_*}\right)x^2-\frac{1}{1-x_*}xy+o(|x,y|^2),\\ \frac{dy}{dt} = \frac{1-d-3x_*}{d+2x_*}x^2-xy+\frac{1}{x_*}y^2+o(|x,y|^2).\end{cases}\tag{19}$$

By Lemma 3.1 in Ref. [41], system (19) can be rewritten as

$$\begin{cases}\frac{dx}{dt} = y,\\ \frac{dy}{dt} = \frac{1-d-3x_*}{d+2x_*}x^2+\left(-1-\frac{2}{1-x_*}+\frac{2}{d+2x_*}\right)xy+o(|x,y|^2).\end{cases}\tag{20}$$

When $d=d_1$, we know that $\frac{3-\sqrt{5}}{2}<x_*<1$, $\frac{1-d-3x_*}{d+2x_*}, -1-\frac{2}{1-x_*}+\frac{2}{d+2x_*}<0$ and therefore the positive equilibrium E_* is a cusp of codimension 2 based on the results in Perko.[40]

For (II) (i), we can get that $0 < x_* < \frac{1}{2}$ when $d = d_2$. Substituting both $d = d_2$ and the conditions in (12) into $\mathrm{tr}(J(E_1))$, we derive

$$\mathrm{tr}(J(E_1)) = \frac{(x_* - 4)(1 - x_*)^2}{(3 - x_*)^2} < 0$$

for $0 < x_* < \frac{1}{2}$ and consequently, the positive equilibrium E_1 is a stable hyperbolic focus or node.

Finally, we turn to part (II) (ii) that the equilibrium E_* is a cusp of codimension 3. In accordance with (20), we know that if $(-1 - \frac{2}{1-x_*} + \frac{2}{d+2x_*}) = 0$, that is, $d = d_2$, the equilibrium $E_*(x_*, (1 - x_*)^2(d + 2x_*)x_*) = (x_*, \frac{2(1-x_*)^3 x_*}{3-x_*})$ is a cusp of codimension at least three. Next, we will show that the codimension of E_* is exactly three. Transforming E_* into the origin by $X = x - x_*, Y = y - \frac{2(1-x_*)^3 x_*}{3-x_*}$ and expressing the resulting system (7) in power series around the origin, we can obtain (for convenience, in every subsequent transformation, we rename X, Y, τ as x, y, t, respectively)

$$\begin{cases} \frac{dx}{dt} = (1 - x_*)x - \frac{3-x_*}{2(1-x_*)^2}y - \frac{1}{2}x^2 + \frac{3-x_*}{2(1-x_*)^3}xy + \frac{x_*^2-2x_*-1}{2(1-x_*)^2x_*}x^3 \\ \qquad + \frac{3-x_*}{4(1-x_*)^3x_*}x^2y - \frac{x_*^3-2x_*^2-x_*-2}{4(1-x_*)^3x_*^2}x^4 + \frac{(3-x_*)(x_*^2-2x_*-1)}{4(1-x_*)^5x_*^2}x^3y \\ \qquad + o(|x, y|^4), \\ \frac{dy}{dt} = \frac{2(1-x_*)^4}{3-x_*}x - (1 - x_*)y - \frac{2(1-x_*)^4}{(3-x_*)x_*}x^2 + \frac{2(1-x_*)}{x_*}xy - \frac{3-x_*}{2(1-x_*)^2x_*}y^2 \\ \qquad + \frac{2(1-x_*)^4}{(3-x_*)x_*^2}x^3 - \frac{2(1-x_*)}{x_*^2}x^2y + \frac{3-x_*}{2(1-x_*)^2x_*^2}xy^2 - \frac{2(1-x_*)^4}{(3-x_*)x_*^3}x^4 \\ \qquad + \frac{2(1-x_*)}{x_*^3}x^3y - \frac{3-x_*}{2(1-x_*)^2x_*^3}x^2y^2 + o(|x, y|^4). \end{cases} \tag{21}$$

Taking a change of coordinates as follows:

$$X = x, Y = (1 - x_*)x - \frac{3 - x_*}{2(1 - x_*)^2}y - \frac{1}{2}x^2 + \frac{3 - x_*}{2(1 - x_*)^3}xy + \frac{x_*^2 - 2x_* - 1}{2(1 - x_*)^2x_*}x^3$$
$$+\frac{3 - x_*}{4(1 - x_*)^3x_*}x^2y - \frac{x_*^3 - 2x_*^2 - x_* - 2}{4(1 - x_*)^3x_*^2}x^4 + \frac{(3 - x_*)(x_*^2 - 2x_* - 1)}{4(1 - x_*)^5x_*^2}x^3y + o(|x, y|^4),$$

system (21) can be expressed by

$$\begin{cases} \frac{dx}{dt} = y, \\ \frac{dy}{dt} = \frac{1-x_*}{2}x^2 + \frac{1-2x_*}{(1-x_*)x_*}y^2 - \frac{2-x_*}{1-x_*}x^3 + \frac{2x_*^2-5x_*-3}{2(1-x_*)^2x_*}x^2y - \frac{2x_*^2-2x_*+1}{(1-x_*)^2x_*^2}xy^2 \\ \qquad + \frac{3-x_*}{2(1-x_*)^2}x^4 - \frac{3(x_*^3-2x_*^2-1)}{2(1-x_*)^3x_*^2}x^3y - \frac{7x_*^3-13x_*^2+4x_*-2}{2(1-x_*)^3x_*^3}x^2y^2 + o(|x, y|^4). \end{cases} \tag{22}$$

Making a time transformation

$$dt = \left(1 - \frac{1 - 2x_*}{(1 - x_*)x_*}x\right)d\tau,$$

we can rewrite system (22) as follows:

$$\begin{cases} \frac{dx}{dt} = y\left(1 - \frac{1-2x_*}{(1-x_*)x_*}x\right), \\ \frac{dy}{dt} = \left(1 - \frac{1-2x_*}{(1-x_*)x_*}x\right)\left\{\frac{1-x_*}{2}x^2 + \frac{1-2x_*}{(1-x_*)x_*}y^2 - \frac{2-x_*}{1-x_*}x^3\right. \\ \quad + \frac{(x_*-3)(2x_*+1)}{2(x_*-1)^2x_*}x^2y - \frac{2x_*^2-2x_*+1}{(1-x_*)^2x_*^2}xy^2 + \frac{3-x_*}{2(1-x_*)^2}x^4 \\ \quad \left. - \frac{3(x_*^3-2x_*^2-1)}{2(1-x_*)^3x_*^2}x^3y - \frac{7x_*^3-13x_*^2+4x_*-2}{2(1-x_*)^3}x^2y^2 + o(|x,y|^4)\right\}. \end{cases} \tag{23}$$

Further, setting

$$X = x, Y = y\left(1 - \frac{1-2x_*}{(1-x_*)x_*}x\right),$$

system (23) continues as

$$\begin{cases} \frac{dx}{dt} = y, \\ \frac{dy}{dt} = \frac{1-x_*}{2}x^2 - \frac{x_*^2-x_*+1}{x_*(1-x_*)}x^3 - \frac{(3-x_*)(1+2x_*)}{2(1-x_*)^2x_*}x^2y - \frac{2(3x_*^2-3x_*+1)}{(1-x_*)^2x_*^2}xy^2 \\ \quad + \frac{3x_*^3-9x_*^2+3x_*+1}{2(1-x_*)^2x_*^2}x^4 + \frac{(6-x_*)(1+x_*)}{2(1-x_*)^2x_*^2}x^3y + \frac{9x_*^2-11x_*+8}{2(1-x_*)^3x_*^2}x^2y^2 + o(|x,y|^4). \end{cases}$$

Finally, noticing $0 < x_* < \frac{1}{2}$ and making the following scalings

$$X = x, Y = \frac{y}{\sqrt{\frac{1-x_*}{2}}}, \tau = \sqrt{\frac{1-x_*}{2}}t,$$

we have

$$\begin{cases} \frac{dx}{dt} = y, \\ \frac{dy}{dt} = x^2 - \frac{2(x_*^2-x_*+1)}{(1-x_*)^2x_*}x^3 + \frac{3x_*^3-9x_*^2+3x_*+1}{(1-x_*)^3x_*^2}x^4 \\ \quad + y\left(-\frac{(3-x_*)(1+2x_*)}{\sqrt{2}(1-x_*)^{\frac{5}{2}}x_*}x^2 + \frac{(6-x_*)(1+x_*)}{\sqrt{2}(1-x_*)^{\frac{5}{2}}x_*^2}x^3\right) \\ \quad + y^2\left(-\frac{2(3x_*^2-3x_*+1)}{(1-x_*)^2x_*^2}x + \frac{9x_*^2-11x_*+8}{2(1-x_*)^3x_*^2}x^2\right) + o(|x,y|^4). \end{cases} \tag{24}$$

Following Proposition 5.3 in Lemontagne et al.,[42] an equivalent system of (24) is given by

$$\begin{cases} \frac{dx}{dt} = y, \\ \frac{dy}{dt} = x^2 + Fx^3y + o(|x,y|^4), \end{cases}$$

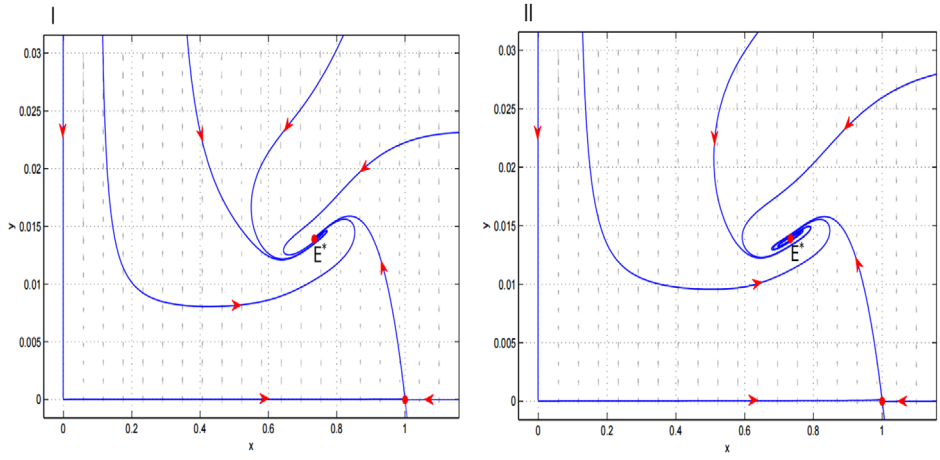

FIGURE 3 The phase portraits of Theorem 4. (I) a stable degenerate node $E^*(\frac{11}{15}, \frac{704}{50625})$ with $d = -\frac{6}{5}, a = \frac{1331}{3375}, \delta = \frac{1}{3}, \beta = \frac{1125}{64}$; (II) a focus of codimension 3, $E^*(\frac{11}{15}, \frac{704}{50625})$ with $d = -\frac{6}{5}, a = \frac{1331}{3375}, \delta = \frac{4}{15}, \beta = \frac{225}{16}$.

where

$$F = \frac{3x_*^3 - 7x_*^2 + 3x_* - 11}{\sqrt{2}(1 - x_*)^{\frac{9}{2}} x_*} < 0$$

for $0 < x_* < \frac{1}{2}$. This indicates that E_* is a cusp of codimension 3 and we complete the proof. □

2.2 | Focus of codimension 3

In this subsection, we study the scenario (II) in Theorem 2. We have the following result.

Theorem 4. *Suppose that the condition (II) in Theorem 2 is satisfied, then system (7) has a unique degenerate positive equilibrium* $E^*(x^*, \frac{\delta}{\beta}x^*) = (\frac{1-d}{3}, \frac{(1-d)(d+2)^3}{81})$. *Furthermore,*

(I) when $\delta \neq \frac{d+2}{3}$, E^* *is a stable (or unstable) degenerate node if* $\delta > \frac{d+2}{3}$ *(or* $\delta < \frac{d+2}{3}$*);*
(II) when $\delta = \frac{d+2}{3}$, E^* *is a nilpotent focus of codimension 3.*

The corresponding phase portraits are given in Figure 3.

Proof. By the condition (II) in Theorem 2, we can obtain that $a = \frac{(1-d)^3}{27}, \frac{\delta}{\beta} = \frac{(2+d)^3}{27}$. Substituting them into $\det(J(E^*))$ and $\mathrm{tr}(J(E^*))$ yields

$$\det(J(E^*)) = 0, \quad \mathrm{tr}(J(E^*)) = \frac{d + 2 - 3\delta}{3}.$$

(I) For $\delta \neq \frac{d+2}{3}$, one can easily get $\mathrm{tr}(J(E^*)) \neq 0$, which indicates that the Jacobian matrix has only one zero eigenvalue. By Theorem 7.1 in Zhang et al.,[7] $E^*(\frac{1-d}{3}, \frac{(1-d)(2+d)^3}{81})$ is a stable (or unstable) degenerate node if $\delta > \frac{d+2}{3}$ (or $\delta < \frac{d+2}{3}$).

Now we turn to the proof of (II). First, setting

$$\text{(i)}\ \ X = x - \frac{1-d}{3}, Y = y - \frac{(1-d)(2+d)^3}{81},$$

and by Taylor expansion, we obtain the following system (for convenience, in every subsequent transformation, we rename X, Y as x, y, respectively):

$$\begin{cases} \frac{dx}{dt} = \frac{d+2}{3}x - \frac{9}{(d+2)^2}y - x^2 + \frac{27}{(d+2)^3}xy - \frac{9}{(d+2)^2}x^3 - \frac{81}{(d-1)(d+2)^3}x^4 \\ \qquad + \frac{729}{(d-1)(d+2)^5}x^3y + o(|x,y|^4), \\ \frac{dy}{dt} = \frac{(d+2)^4}{81}x - \frac{d+2}{3}y + \frac{(d+2)^4}{27(d-1)}x^2 - \frac{2(d+2)}{d-1}xy + \frac{27}{(d-1)(d+2)^2}y^2 \\ \qquad + \frac{(d+2)^4}{9(d-1)^2}x^3 - \frac{6(d+2)}{(d-1)^2}x^2y + \frac{81}{(d-1)^2(d+2)^2}xy^2 + \frac{(d+2)^4}{3(d-1)^3}x^4 \\ \qquad - \frac{18(d+2)}{(d-1)^3}x^3y + \frac{243}{(d-1)^3(d+2)^2}x^2y^2 + o(|x,y|^4), \end{cases}$$

where a, δ, β are replaced with expressions for d.

Second, we let

$$\text{(ii)}\ \ x = \frac{1}{2(d+2)^3}X + \frac{3}{4(d+2)^4}Y,\ \ y = \frac{1}{54}X - \frac{1}{36(d+2)}Y,$$

and get the following system with a linear part in the Jordan canonical form:

$$\begin{cases} \frac{dx}{dt} = y - \frac{3}{4(d+2)^4}xy + \frac{9(d+5)}{8(d-1)(d+2)^5}y^2 - \frac{9}{8(d+2)^8}x^3 - \frac{81}{16(d+2)^9}x^2y \\ \qquad + \frac{27\left(\frac{4(d+2)^3}{(d-1)^2}-9\right)}{32(d+2)^{10}}xy^2 + \frac{81\left(\frac{4(d+2)^3}{(d-1)^2}-3\right)}{64(d+2)^{11}}y^3 + \frac{27}{16(d+2)^{12}}x^4 + \frac{81(d-4)}{16(d-1)(d+2)^{13}}x^3y \\ \qquad + \frac{81\left(2(d+2)^4-27(d-1)^2\right)}{32(d-1)^3(d+2)^{14}}x^2y^2 + \frac{243(d+5)(4d^3+9d^2+33d+8)}{64(d-1)^3(d+2)^{15}}xy^3 \\ \qquad + \frac{729(4d^4+29d^3+87d^2+155d+49)}{256(d-1)^3(d+2)^{16}}y^4 + o(|x,y|^4), \\ \frac{dy}{dt} = -\frac{1}{2(d+2)^3}xy - \frac{9(d+1)}{4(d-1)(d+2)^4}y^2 - \frac{3}{4(d+2)^7}x^3 - \frac{27}{8(d+2)^8}x^2y + \frac{9\left(-\frac{4(d+2)^3}{(d-1)^2}-9\right)}{16(d+2)^9}xy^2 \\ \qquad + \frac{27\left(-\frac{4(d+2)^3}{(d-1)^2}-3\right)}{32(d+2)^{10}}y^3 + \frac{9}{8(d+2)^{11}}x^4 + \frac{27(d-4)}{8(d-1)(d+2)^{12}}x^3y \\ \qquad + \frac{27\left(-2(d+2)^4-27(d-1)^2\right)}{16(d-1)^3(d+2)^{13}}x^2y^2 - \frac{81(4d^4+35d^3+114d^2+83d+88)}{32(d-1)^3(d+2)^{14}}xy^3 \\ \qquad + \frac{243\left(-4(d+2)^4-3(d-1)^2(d+5)\right)}{128(d-1)^3(d+2)^{15}}y^4 + o(|x,y|^4). \end{cases}$$

Making the following transformations:

$$\text{(iii)}\ \ x = X - \frac{3(2d+1)}{4(d-1)(d+2)^4}X^2,\ \ y = Y - \frac{9(d+1)}{4(d-1)(d+2)^4}XY - \frac{9(d+5)}{8(d-1)(d+2)^5}Y^2,$$

we change the above system to

$$\begin{cases} \dfrac{dx}{dt} = y + a_{30}^* x^3 + a_{21}^* x^2 y + a_{12}^* xy^2 + a_{03}^* y^3 + a_{40}^* x^4 + a_{31}^* x^3 y + a_{22}^* x^2 y^2 \\ \qquad + a_{13}^* xy^3 + a_{04}^* y^4 + o(|x,y|^4), \\ \dfrac{dy}{dt} = b_{11}^* xy + b_{30}^* x^3 + b_{21}^* x^2 y + b_{12}^* xy^2 + b_{03}^* y^3 + b_{40}^* x^4 + b_{31}^* x^3 y \\ \qquad + b_{22}^* x^2 y^2 + b_{13}^* xy^3 + b_{04}^* y^4 + o(|x,y|^4), \end{cases} \tag{25}$$

in which

$$a_{30}^* = -\frac{9}{8(d+2)^8},\ \ a_{21}^* = \frac{9\left(5d^2+5d+17\right)}{16(d-1)(d+2)^9},$$

$$a_{12}^* = -\frac{27\left(d^3+27d^2+33d+47\right)}{32(d-1)^2(d+2)^{10}},\ \ a_{03}^* = \frac{81\left(2d^3-3d^2-36d-71\right)}{64(d-1)^2(d+2)^{11}},$$

$$a_{40}^* = \frac{27(4d-1)}{32(d-1)(d+2)^{12}},\ \ a_{31}^* = \frac{27\left(14d^3+84d^2-21d+31\right)}{64(d-1)^2(d+2)^{13}},$$

$$a_{22}^* = -\frac{243\left(7d^4+39d^3+165d^2+83d+30\right)}{128(d-1)^3(d+2)^{14}},$$

$$a_{13}^* = -\frac{243\left(14d^4+109d^3+453d^2+547d+173\right)}{256(d-1)^3(d+2)^{15}},$$

$$a_{04}^* = -\frac{2187\left(d^4+16d^3+66d^2+104d+29\right)}{512(d-1)^3(d+2)^{16}},\ \ b_{11}^* = -\frac{1}{2(d+2)^3},$$

$$b_{30}^* = -\frac{3}{4(d+2)^7},\ \ b_{21}^* = \frac{3\left(2d^2-4d+11\right)}{8(d-1)(d+2)^8},$$

$$b_{12}^* = \frac{9\left(13d^3+33d^2+57d+5\right)}{16(d-1)^2(d+2)^9},\ \ b_{03}^* = \frac{27(d+5)^2(2d+1)}{32(d-1)^2(d+2)^{10}},$$

$$b_{40}^* = \frac{9(5d-2)}{16(d-1)(d+2)^{11}},\ \ b_{31}^* = \frac{27(11d-23)}{32(d-1)(d+2)^{12}},$$

$$b_{22}^* = \frac{27\left(53d^4+250d^3+219d^2+544d-94\right)}{64(d-1)^3(d+2)^{13}},$$

$$b_{13}^* = \frac{243\left(13d^4+88d^3+204d^2+284d+59\right)}{128(d-1)^3(d+2)^{14}},$$

$$b_{04}^* = \frac{243\left(11d^3+69d^2+225d+127\right)}{256(d-1)^3(d+2)^{14}}.$$

By straightforward computation, we have

$$b_{11}^* b_{30}^* = \frac{3}{8(d+2)^{10}} \neq 0,$$

which indicates that there is a small neighborhood of (0,0) in which system (25) is locally topologically equivalent to

$$\begin{cases} \frac{dx}{dt} = y, \\ \frac{dy}{dt} = b_{11}^* xy + b_{30}^* x^3 + (b_{21}^* + 3a_{30}^*)x^2 y + (b_{40}^* - b_{11}^* a_{30}^*)x^4 \\ \qquad + (4a_{40}^* + b_{31}^* + \frac{1}{3}b_{11}^* a_{21}^* + \frac{1}{6}b_{11}^* b_{12}^*)x^3 y + o(|x,y|^4). \end{cases} \tag{26}$$

In addition, $-2 < d < 1$ leads to

$$5b_{30}^*(b_{21}^* + b_{30}^*) - 3b_{11}^*(b_{40}^* - b_{11}^* a_{30}^*) = \frac{9(d^2 + 43d - 53)}{16(d-1)(d+2)^{15}} \neq 0,$$

and

$$b_{30}^* = -\frac{3}{4(d+2)^7} < 0, \quad b_{11}^{*2} + 8b_{30}^* = \frac{d-22}{4(d+2)^7} < 0.$$

By Lemma 3.1 in Cai et al.,[43] we can conclude that the equilibrium (0,0) of system (26) is a degenerate focus of codimension 3. Correspondingly, the unique degenerate positive equilibrium $E^*(\frac{1-d}{3}, \frac{(1-d)(2+d)^3}{81})$ of system (7) is a degenerate Bogdanov–Takens singularity (focus case) of codimension 3. □

3 | BIFURCATION ANALYSIS

Based on Theorem 3, system (7) may exhibit Bogdanov–Takens bifurcation of codimensions 2 and 3 around E_* with a certain range of parameter values. Because the analysis of degenerate cusp-type Bogdanov–Takens bifurcation of codimension 3 in system (7) with $d = 0$ was not provided in the studies of Huang et al.[35] and Li and Xiao,[33] here we present the bifurcation results for the sake of completeness. We will investigate the codimension of Bogdanov–Takens bifurcation including two and three.

3.1 | Degenerate cusp-type Bogdanov–Takens bifurcation of codimension 2

We first concentrate on the cusp type of Bogdanov–Takens bifurcation of codimension 2. We have the following result.

Theorem 5. *Assume that the conditions (III) in Theorem 2 and (12) are satisfied and $d = d_1$, then system (7) has a cusp $E_*(x_*, (2-x_*)(1-x_*)^3 x_*)$ of codimension 2 (i.e., Bogdanov–Takens*

bifurcation singularity). Choosing a and δ as bifurcation parameters, system (7) undergoes Bogdanov–Takens bifurcation of codimension 2 in a small neighborhood of the unique positive equilibrium $E_*(x_*, (2-x_*)(1-x_*)^3x_*)$. Therefore, there exist some parameter values such that system (7) has an unstable limit cycle, and there exist some other parameter values such that system (7) has an unstable homoclinic loop.

Proof. Taking a and δ as bifurcation parameters, we have

$$\begin{cases} \frac{dx}{dt} = x(1-x) - \frac{xy}{x^2+dx+a+\lambda_1}, \\ \frac{dy}{dt} = y(\delta + \lambda_2 - \frac{\beta y}{x}), \end{cases} \tag{27}$$

where $d = x_*^2 - 5x_* + 2, a = -x_*^2(x_*^2 - 3x_* + 1), \delta = 1 - x_*, \beta = \frac{1}{(2-x_*)(1-x_*)^2}$ by $d = d_1$, the conditions given in (12) and $\lambda = (\lambda_1, \lambda_2) \sim (0,0)$. We focus on the phase portraits of system (27) when x and y lie in a small neighborhood of the interior equilibrium $E_*(x_*, y_*)$.

We shift the equilibrium $E_*(x_*, (2-x_*)(1-x_*)^3x_*)$ of system (27) when $\lambda = 0$ to the origin. Letting $X = x - x_*, Y = y - (2-x_*)(1-x_*)^3x_*$ and by the Taylor expansion, system (27) can be represented by (for convenience, in every subsequent transformation, we rename X, Y, τ as x, y, t, respectively)

$$\begin{cases} \frac{dx}{dt} = \widehat{a}_{00} + \widehat{a}_{10}x + \widehat{a}_{01}y + \widehat{a}_{20}x^2 + \widehat{a}_{11}xy + \widehat{L}_1(x, y, \lambda_1, \lambda_2), \\ \frac{dy}{dt} = \widehat{b}_{00} + \widehat{b}_{10}x + \widehat{b}_{01}y + \widehat{b}_{20}x^2 + \widehat{b}_{11}xy + \widehat{b}_{02}y^2 + \widehat{L}_2(x, y, \lambda_1, \lambda_2), \end{cases}$$

where $\widehat{L}_1(x, y, \lambda_1, \lambda_2), \widehat{L}_2(x, y, \lambda_1, \lambda_2)$ are C^∞ function as least of third order with respect to x, y. Their coefficients depend smoothly on λ_1 and λ_2, and

$$\widehat{a}_{00} = \frac{\lambda_1(1-x_*)x_*}{\lambda_1 + (2-x_*)x_*(1-x_*)^2},$$

$$\widehat{a}_{10} = \frac{(2-x_*)x_*(1-x_*)^3\big((2-x_*)(1-x_*)x_*^2 - \lambda_1\big)}{\big(\lambda_1 + (2-x_*)x_*(1-x_*)^2\big)^2} - 2x_* + 1,$$

$$\widehat{a}_{01} = \frac{x_*}{-\lambda_1 - (2-x_*)x_*(1-x_*)^2},$$

$$\widehat{a}_{20} = \frac{(2-x_*)(1-x_*)^3x_*\big((2-x_*)(1-x_*)^3x_*^2 - \lambda_1(2-(2-x_*)x_*)\big)}{\big(-\lambda_1 - (2-x_*)x_*(1-x_*)^2\big)^3} - 1,$$

$$\widehat{a}_{11} = \frac{(2-x_*)(1-x_*)x_*^2 - \lambda_1}{\big(\lambda_1 + (2-x_*)x_*(1-x_*)^2\big)^2},\ \widehat{b}_{00} = \lambda_2(2-x_*)(1-x_*)^3x_*,$$

$$\widehat{b}_{10} = (2-x_*)(1-x_*)^4,\ \widehat{b}_{01} = \lambda_2 + x_* - 1, \widehat{b}_{20} = -\frac{(2-x_*)(1-x_*)^4}{x_*},$$

$$\widehat{b}_{11} = \frac{2(1-x_*)}{x_*},\ \widehat{b}_{02} = -\frac{1}{(2-x_*)(1-x_*)^2x_*}.$$

Using the transformation $X = x, Y = \widehat{a}_{00} + \widehat{a}_{10}x + \widehat{a}_{01}y + \widehat{a}_{20}x^2 + \widehat{a}_{11}xy + \widehat{L}_1(x, y, \lambda_1, \lambda_2)$, we obtain

$$\begin{cases} \frac{dx}{dt} = y, \\ \frac{dy}{dt} = \widehat{c}_{00} + \widehat{c}_{10}x + \widehat{c}_{01}y + \widehat{c}_{20}x^2 + \widehat{c}_{11}xy + \widehat{c}_{02}y^2 + \widehat{L}_3(x, y, \lambda_1, \lambda_2), \end{cases}$$

where $\widehat{L}_3(x, y, \lambda_1, \lambda_2)$ is C^∞ function as least of third order with respect to x, y. The coefficients depend smoothly on λ_1 and λ_2, and

$$\widehat{c}_{00} = \frac{\widehat{a}_{00}^2\widehat{b}_{02}}{\widehat{a}_{01}} - \widehat{a}_{00}\widehat{b}_{01} + \widehat{a}_{01}\widehat{b}_{00},$$

$$\widehat{c}_{10} = \widehat{a}_{10}\left(\frac{2\widehat{a}_{00}\widehat{b}_{02}}{\widehat{a}_{01}} - \widehat{b}_{01}\right) + \widehat{a}_{11}\left(\widehat{b}_{00} - \frac{\widehat{a}_{00}^2\widehat{b}_{02}}{\widehat{a}_{01}^2}\right) + \widehat{a}_{01}\widehat{b}_{10} - \widehat{a}_{00}\widehat{b}_{11},$$

$$\widehat{c}_{01} = -\frac{\widehat{a}_{00}\left(\widehat{a}_{11} + 2\widehat{b}_{02}\right)}{\widehat{a}_{01}} + \widehat{a}_{10} + \widehat{b}_{01},$$

$$\widehat{c}_{20} = -\widehat{a}_{20}\widehat{b}_{01} + \frac{\left(2\widehat{a}_{00}\widehat{a}_{20}\widehat{a}_{01}^2 + (\widehat{a}_{01}\widehat{a}_{10} - \widehat{a}_{00}\widehat{a}_{11})^2\right)\widehat{b}_{02}}{\widehat{a}_{01}^3} + \widehat{a}_{11}\widehat{b}_{10} - \widehat{a}_{10}\widehat{b}_{11} + \widehat{a}_{01}\widehat{b}_{20},$$

$$\widehat{c}_{11} = -\frac{(\widehat{a}_{01}\widehat{a}_{10} - \widehat{a}_{00}\widehat{a}_{11})\left(\widehat{a}_{11} + 2\widehat{b}_{02}\right)}{\widehat{a}_{01}^2} + 2\widehat{a}_{20} + \widehat{b}_{11},$$

$$\widehat{c}_{02} = \frac{\widehat{a}_{11} + \widehat{b}_2}{\widehat{a}_{01}}.$$

With a change of time $dt = (1 - \widehat{c}_{02}x)d\tau$, we get

$$\begin{cases} \frac{dx}{dt} = y(1 - \widehat{c}_{02}x), \\ \frac{dy}{dt} = (1 - \widehat{c}_{02}x)(\widehat{c}_{00} + \widehat{c}_{10}x + \widehat{c}_{01}y + \widehat{c}_{20}x^2 + \widehat{c}_{11}xy + \widehat{c}_{02}y^2 \\ \qquad + \widehat{L}_3(x, y, \lambda_1, \lambda_2)). \end{cases} \tag{28}$$

Letting $X = x, Y = y(1 - \widehat{c}_{02}x)$, a new system equivalent to (28) can be derived as follows:

$$\begin{cases} \frac{dx}{dt} = y, \\ \frac{dy}{dt} = \widehat{d}_{00} + \widehat{d}_{10}x + \widehat{d}_{01}y + \widehat{d}_{20}x^2 + \widehat{d}_{11}xy + \widehat{L}_4(x, y, \lambda_1, \lambda_2), \end{cases}$$

where $\widehat{L}_4(x, y, \lambda_1, \lambda_2)$ is C^∞ function as least of third order with respect to x, y, and

$$\widehat{d}_{00} = \widehat{c}_{00},\ \widehat{d}_{10} = \widehat{c}_{10} - 2\widehat{c}_{00}\widehat{c}_{02},\ \widehat{d}_{01} = \widehat{c}_{01},$$
$$\widehat{d}_{20} = \widehat{c}_{00}\widehat{c}_{02}^2 - 2\widehat{c}_{10}\widehat{c}_{02} + \widehat{c}_{20},\ \widehat{d}_{11} = \widehat{c}_{11} - \widehat{c}_{01}\widehat{c}_{02}.$$

Letting $X = x + \frac{\widehat{d}_{10}}{2\widehat{d}_{20}}, Y = y$, we obtain

$$\begin{cases} \frac{dx}{dt} = y, \\ \frac{dy}{dt} = \widehat{e}_{00} + \widehat{e}_{01}y + \widehat{e}_{20}x^2 + \widehat{e}_{11}xy + \widehat{L}_5(x, y, \lambda_1, \lambda_2), \end{cases}$$

where $\widehat{L}_5(x, y, \lambda_1, \lambda_2)$ is C^∞ function as least of third order with respect to x, y with coefficients smoothly dependent on λ_1 and λ_2, and

$$\widehat{e}_{00} = \widehat{d}_{00} - \frac{\widehat{d}_{10}^2}{4\widehat{d}_{20}},\ \widehat{e}_{01} = \widehat{d}_{01} - \frac{\widehat{d}_{10}\widehat{d}_{11}}{2\widehat{d}_{20}},$$
$$\widehat{e}_{20} = \widehat{d}_{20},\ \widehat{e}_{11} = \widehat{d}_{11}.$$

With $X = \frac{\widehat{e}_{11}^2}{\widehat{e}_{20}}x, Y = \frac{\widehat{e}_{11}^3}{\widehat{e}_{20}^2}y, \tau = \frac{\widehat{e}_{20}}{\widehat{e}_{11}}t$, it produces that

$$\begin{cases} \frac{dx}{dt} = y, \\ \frac{dy}{dt} = \widehat{\mu}_1 + \widehat{\mu}_2 y + x^2 + xy + \widehat{L}_6(x, y, \lambda_1, \lambda_2), \end{cases} \tag{29}$$

where $\widehat{L}_6(x, y, \lambda_1, \lambda_2)$ is C^∞ function as least of third order with respect to x, y and

$$\widehat{\mu}_1 = \frac{\widehat{e}_{00}\widehat{e}_{11}^4}{\widehat{e}_{20}^3},\ \widehat{\mu}_2 = \frac{\widehat{e}_{01}\widehat{e}_{11}}{\widehat{e}_{20}}.$$

Finally, we expand $\widehat{\mu}_1$ and $\widehat{\mu}_2$ in terms of λ_1 and λ_2 as follows:

$$\widehat{\mu}_1 = \widehat{m}_{10}\lambda_1 + \widehat{m}_{01}\lambda_2 + \widehat{m}_{20}\lambda_1^2 + \widehat{m}_{11}\lambda_1\lambda_2 + \widehat{m}_{02}\lambda_2^2 + o(|\lambda_1, \lambda_2|^2),$$
$$\widehat{\mu}_2 = \widehat{n}_{10}\lambda_1 + \widehat{n}_{01}\lambda_2 + \widehat{n}_{20}\lambda_1^2 + \widehat{n}_{11}\lambda_1\lambda_2 + \widehat{n}_{02}\lambda_2^2 + o(|\lambda_1, \lambda_2|^2),$$

in which

$$\widehat{m}_{10} = \frac{(x_* - 4)^4}{(x_* - 2)^2(x_* - 1)^3},\ \widehat{m}_{01} = -\frac{(x_* - 4)^4 x_*}{(x_* - 2)(x_* - 1)^2},$$
$$\widehat{m}_{20} = \frac{2(x_* - 4)^3\left(4x_*^3 - 27x_*^2 + 36x_* - 4\right)}{(x_* - 2)^3(x_* - 1)^6 x_*},$$
$$\widehat{m}_{11} = -\frac{(x_* - 4)^3\left(16x_*^4 - 115x_*^3 + 200x_*^2 - 106x_* + 32\right)}{(x_* - 2)^2(x_* - 1)^5 x_*},$$

$$\widehat{m}_{02} = \frac{(x_*-4)^3\left(32x_*^4-244x_*^3+511x_*^2-386x_*+120\right)}{4(x_*-2)(x_*-1)^4},$$

$$\widehat{n}_{10} = -\frac{(x_*-4)((x_*-3)x_*+1)}{(x_*-2)(x_*-1)^3x_*},$$

$$\widehat{n}_{01} = \frac{(x_*-4)(x_*(2x_*-7)+2)}{2(x_*-1)^2},$$

$$\widehat{n}_{20} = \frac{-12x_*^5+129x_*^4-478x_*^3+741x_*^2-484x_*+116}{2(x_*-2)^2(x_*-1)^6x_*^2},$$

$$\widehat{n}_{11} = \frac{12x_*^6-133x_*^5+519x_*^4-882x_*^3+708x_*^2-295x_*+50}{(x_*-2)(x_*-1)^5x_*^2},$$

$$\widehat{n}_{02} = \frac{-6x_*^6+68x_*^5-275x_*^4+492x_*^3-419x_*^2+179x_*-30}{(x_*-1)^4x_*}.$$

□

In view of

$$\left|\frac{\partial(\widehat{\mu}_1,\widehat{\mu}_2)}{\partial(\lambda_1,\lambda_2)}\right|_{\lambda=0} = -\frac{(x_*-4)^5x_*}{2(x_*-2)^2(x_*-1)^5} < 0$$

for $\frac{3-\sqrt{5}}{2} < x_* < \frac{1}{2}$, system (29) (i.e., (7)) undergoes Bogdanov–Takens bifurcation of codimension 2 when (λ_1,λ_2) changes in a small neighborhood of (0,0) based on the results of Bogdanov[44] and Takens.[45]

Furthermore, according to the results of Perko,[40] the local representation of bifurcation curves around (0,0) can be written by the following:

(i) The saddle-node bifurcation curve is

$$\mathrm{SN} = \{(\widehat{\mu}_1,\widehat{\mu}_2)|\widehat{\mu}_1 = 0, \widehat{\mu}_2 \neq 0\}.$$

(ii) The Hopf bifurcation curve is

$$\mathrm{H} = \{(\widehat{\mu}_1,\widehat{\mu}_2)|\widehat{\mu}_2 = \sqrt{-\widehat{\mu}_1}, \widehat{\mu}_1 < 0\}.$$

(iii) The homoclinic bifurcation curve is

$$\mathrm{HL} = \{(\widehat{\mu}_1,\widehat{\mu}_2)|\widehat{\mu}_2 = \frac{5}{7}\sqrt{-\widehat{\mu}_1}, \widehat{\mu}_1 < 0\}.$$

3.2 | Degenerate cusp-type Bogdanov–Takens bifurcation of codimension 3

Next, we study the cusp-type Bogdanov–Takens bifurcation of codimension 3. For system (7), we select a, δ, and β as bifurcation parameters and have

$$\begin{cases} \frac{dx}{dt} = x(1-x) - \frac{xy}{x^2+dx+a+\lambda_1}, \\ \frac{dy}{dt} = y(\delta + \lambda_2 - \frac{(\beta+\lambda_3)y}{x}), \end{cases} \tag{30}$$

in which $a, \delta, \beta > 0$, $d > -2\sqrt{a}$, and $\lambda = (\lambda_1, \lambda_2, \lambda_3) \sim (0,0,0)$. We aim at transforming (30) to a universal unfolding of a cusp-type degenerate Bogdanov–Takens bifurcation of codimension 3 as

$$\begin{cases} \frac{dx}{dt} = y, \\ \frac{dy}{dt} = \nu_1 + \nu_2 y + \nu_3 xy + x^2 \pm x^3 y + M(x,y,\varepsilon), \end{cases} \tag{31}$$

where

$$\begin{aligned} M(x,y,\varepsilon) = {} & y^2 O(|x,y|^2) + O(|x,y|^5) + O(\varepsilon)(O(y^2) + O(|x,y|^3)) \\ & + O(\varepsilon^2) O(|x,y|) \end{aligned} \tag{32}$$

with a series of near-identity transformations and $|\frac{\partial(\nu_1,\nu_2,\nu_3)}{\partial(\lambda_1,\lambda_2,\lambda_3)}|_{\lambda=0} \neq 0$. This indicates that system (30) (i.e., system (7)) undergoes a Bogdanov–Takens bifurcation of codimension 3. We have the following theorem.

Theorem 6. *Assume that the conditions (III) in Theorem 2 and (12) are satisfied and $d = d_2$, then system (7) admits a cusp $E_*(x_*, \frac{2(x_*-1)^3 x_*}{x_*-3})$ of codimension 3. If we take a, δ, and β as bifurcation parameters, then system (7) undergoes Bogdanov–Takens bifurcation of codimension 3 in a small neighborhood of $E_*(x_*, \frac{2(x_*-1)^3 x_*}{x_*-3})$. Therefore, system (7) exhibits the coexistence of an unstable homoclinic loop and a stable limit cycle, coexistence of two limit cycles (the inner is stable and the outer is unstable), and a semistable limit cycle for different sets of parameters.*

Proof. In the first step, we transform the equilibrium $E_*(x_*, \frac{2(x_*-1)^3 x_*}{x_*-3})$ of system (30) when $\lambda = 0$ to the origin by the transformation $X = x - x_*, Y = y - \frac{2(x_*-1)^3 x_*}{x_*-3}$ and expand the resulting system in power series around the origin. System (30) continues as (again, in every subsequent transformation we rename X, Y, τ as x, y, t, respectively)

$$\begin{cases} \frac{dx}{dt} = \overline{a}_{00} + \overline{a}_{10}x + \overline{a}_{01}y + \overline{a}_{20}x^2 + \overline{a}_{11}xy + \overline{a}_{30}x^3 + \overline{a}_{21}x^2 y + \overline{a}_{40}x^4 \\ \qquad + \overline{a}_{31}x^3 y + o(|x,y|^4), \\ \frac{dy}{dt} = \overline{b}_{00} + \overline{b}_{10}x + \overline{b}_{01}y + \overline{b}_{20}x^2 + \overline{b}_{11}xy + \overline{b}_{02}y^2 + \overline{b}_{30}x^3 + \overline{b}_{21}x^2 y \\ \qquad + \overline{b}_{12}xy^2 + \overline{b}_{40}x^4 + \overline{b}_{31}x^3 y + \overline{b}_{22}x^2 y^2 + o(|x,y|^4), \end{cases} \tag{33}$$

in which

$$\overline{a}_{00} = \frac{\lambda_1(x_*-3)(x_*-1)x_*}{2(x_*-1)^2 x_* - \lambda_1(x_*-3)},$$

$$\overline{a}_{10} = \frac{2x_*(x_*-1)^3\left(2(x_*-1)x_*^2-\lambda_1(x_*-3)\right)}{\left(\lambda_1(x_*-3)-2(x_*-1)^2x_*\right)^2}-2x_*+1,$$

$$\overline{a}_{01} = \frac{(x_*-3)x_*}{2(x_*-1)^2x_*-\lambda_1(x_*-3)},$$

$$\overline{a}_{20} = \frac{4(x_*-1)^6x_*^3-2\lambda_1(x_*-3)(x_*-2)(x_*-1)^3x_*(x_*+1)}{\left(2(x_*-1)^2x_*-\lambda_1(x_*-3)\right)^3}-1,$$

$$\overline{a}_{11} = \frac{(x_*-3)\left(2(x_*-1)x_*^2-\lambda_1(x_*-3)\right)}{\left(\lambda_1(x_*-3)-2(x_*-1)^2x_*\right)^2},$$

$$\overline{a}_{30} = \frac{1}{\left(\lambda_1(x_*-3)-2(x_*-1)^2x_*\right)^4}\{2(x_*-1)^3x_*(4(x_*-1)^3x_*^2((x_*-2)x_*$$
$$-1)-4\lambda_1(x_*-1)(x_*^3-3x_*^2+x_*-1)(x_*-3)+\lambda_1^2(x_*-3)^3)\},$$

$$\overline{a}_{21} = \frac{(x_*-3)\left(2(x_*-1)^3x_*^2-\lambda_1(x_*-3)(x_*-2)(x_*+1)\right)}{\left(2(x_*-1)^2x_*-\lambda_1(x_*-3)\right)^3},$$

$$\overline{a}_{40} = \frac{1}{\left(2(x_*-1)^2x_*-\lambda_1(x_*-3)\right)^5}\{8x_*^3(x_*((x_*-2)x_*-1)-2)(x_*-1)^7$$
$$+2\lambda_1x_*(\lambda_1\left(x_*^2-4x_*+3\right)^3\left(x_*^2+x_*-4\right)-4(x_*-3)(x_*-1)^5$$
$$\times((x_*-1)x_*((x_*-1)x_*-5)-2)\},$$

$$\overline{a}_{31} = \frac{1}{\left(\lambda_1(x_*-3)-2(x_*-1)^2x_*\right)^4}\{(x_*-3)(4(x_*-1)^3x_*^2((x_*-2)x_*-1)$$
$$-4\lambda_1(x_*-1)\left(x_*^3-3x_*^2+x_*-1\right)(x_*-3)+\lambda_1^2(x_*-3)^3)\},$$

$$\overline{b}_{00} = \frac{2\lambda_2(x_*-3)(x_*-1)^3x_*-4\lambda_3(x_*-1)^6x_*}{(x_*-3)^2},$$

$$\overline{b}_{10} = \frac{2(x_*-1)^4\left(2\lambda_3(x_*-1)^2-x_*+3\right)}{(x_*-3)^2},$$

$$\overline{b}_{01} = \lambda_2-\frac{4\lambda_3(x_*-1)^3}{x_*-3}+x_*-1,$$

$$\overline{b}_{20} = \frac{2(x_*-1)^4\left(-2\lambda_3(x_*-1)^2+x_*-3\right)}{(x_*-3)^2x_*},$$

$$\overline{b}_{11} = \frac{2(x_*-1)\left(2\lambda_3(x_*-1)^2-x_*+3\right)}{(x_*-3)x_*},\ \overline{b}_{02} = -\frac{\lambda_3-\frac{x_*-3}{2(x_*-1)^2}}{x_*},$$

$$\overline{b}_{30} = \frac{2(x_*-1)^4\left(2\lambda_3(x_*-1)^2-x_*+3\right)}{(x_*-3)^2x_*^2},$$

$$\bar{b}_{21} = \frac{2\left(x_*^2 - 2\lambda_3(x_* - 1)^3 - 4x_* + 3\right)}{(x_* - 3)x_*^2},$$

$$\bar{b}_{12} = \frac{\lambda_3 - \frac{x_* - 3}{2(x_* - 1)^2}}{x_*^2},\ \bar{b}_{40} = \frac{2(x_* - 1)^4\left(-2\lambda_3(x_* - 1)^2 + x_* - 3\right)}{(x_* - 3)^2 x_*^3},$$

$$\bar{b}_{31} = \frac{2(x_* - 1)\left(2\lambda_3(x_* - 1)^2 - x_* + 3\right)}{(x_* - 3)x_*^3},\ \bar{b}_{22} = -\frac{\lambda_3 - \frac{x_* - 3}{2(x_* - 1)^2}}{x_*^3}.$$

It should be noted that $\bar{a}_{00} = \bar{b}_{00} = 0$ and system (33) is simplified as system (21) when $\lambda = 0$.

Making the transformation

$$\begin{aligned} X &= x, \\ Y &= \bar{a}_{00} + \bar{a}_{10}x + \bar{a}_{01}y + \bar{a}_{20}x^2 + \bar{a}_{11}xy + \bar{a}_{30}x^3 + \bar{a}_{21}x^2y + \bar{a}_{40}x^4 \\ &\quad + \bar{a}_{31}x^3y + o(|x, y|^4), \end{aligned}$$

we have

$$\begin{aligned} \frac{dx}{dt} &= y, \\ \frac{dy}{dt} &= \bar{c}_{00} + \bar{c}_{10}x + \bar{c}_{01}y + \bar{c}_{20}x^2 + \bar{c}_{11}xy + \bar{c}_{02}y^2 + \bar{c}_{30}x^3 + \bar{c}_{21}x^2y \\ &\quad + \bar{c}_{12}xy^2 + \bar{c}_{40}x^4 + \bar{c}_{31}x^3y + \bar{c}_{22}x^2y^2 + o(|x, y|^4), \end{aligned} \tag{34}$$

in which

$$\bar{c}_{00} = (x_* - 1)x_*\left(\lambda_2 - \frac{2\lambda_3(x_* - 1)^3}{x_* - 3}\right) + \frac{1}{2}\lambda_1\left(2\lambda_3(x_* - 1)^2 - x_* + 3\right),$$

$$\bar{c}_{10} = \frac{\lambda_1\left(2\lambda_3(x_* - 1)^2 - x_* + 3\right)}{x_* - 1} + \frac{(2x_* - 1)\left(\lambda_2(x_* - 3) - 2\lambda_3(x_* - 1)^3\right)}{x_* - 3},$$

$$\begin{aligned} \bar{c}_{01} &= \lambda_2 - \frac{4\lambda_3(x_* - 1)^3}{x_* - 3} + \frac{2x_*(x_* - 1)^2}{2(x_* - 1)^2x_* - \lambda_1(x_* - 3)} \\ &\quad + \frac{\lambda_1\left(2\lambda_3(x_* - 1)^2 - x_* + 3\right)}{(x_* - 1)x_*} - 1, \end{aligned}$$

$$\bar{c}_{20} = \lambda_2 + \lambda_1\lambda_3 + \frac{1}{2}\left(-\frac{2\lambda_3(x_* - 1)^3}{x_* - 3} - x_* + 1\right) - \frac{\lambda_1(x_* - 3)}{2(x_* - 1)^2},$$

$$\begin{aligned} \bar{c}_{11} &= \frac{\lambda_1}{(x_* - 1)^2x_*^2(\lambda_1(x_* - 3) - 2(x_* - 1)^2x_*)^2}\Big\{\lambda_1(-(x_* - 4)x_* \\ &\quad \times \left(x_*^2 - 4x_* + 3\right)^2 - \lambda_1(x_* - 3)^3) + 2(x_* - 3)x_*^2((x_* - 3)x_* + 3) \end{aligned}$$

$$\times (x_*-1)^3 + 2\lambda_3\left(\lambda_1(x_*-3)(x_*-1) - 2(x_*-1)^3 x_*\right)^2\Big\},$$

$$\bar{c}_{02} = \frac{2(x_*-1)^2 x_* - \lambda_1(x_*-3)}{(x_*-3)x_*}\left(\frac{(x_*-3)\left(2(x_*-1)x_*^2 - \lambda_1(x_*-3)\right)}{\left(\lambda_1(x_*-3) - 2(x_*-1)^2 x_*\right)^2} - \frac{\lambda_3 - \frac{x_*-3}{2(x_*-1)^2}}{x_*}\right),$$

$$\bar{c}_{30} = \frac{1}{2(x_*-3)(x_*-1)x_*^3(2(x_*-1)^2x_* - \lambda_1(x_*-3))}\{(4(x_*-2) \times (x_*-1)^2 x_*^4 + \lambda_1(x_*-3)\left(-2(x_*-2)x_*^3 - \lambda_1(x_*-3)(x_*-1)\right)) \times \left(2\lambda_3(x_*-1)^2 - x_* + 3\right)\},$$

$$\bar{c}_{21} = \frac{1}{(x_*-3)(x_*-1)^2x_*^3(2(x_*-1)^2x_* - \lambda_1(x_*-3))^3}\{-\lambda_1^3(x_*-3)^3 \times (x_*-1)^2\left(2\lambda_3(x_*-1)^2 - x_* + 3\right)x_*(x_*+6) + \lambda_1^4(x_*-3)^4 \times \left(2\lambda_3(x_*-1)^2 - x_* + 3\right) + 4(x_*-1)^6x_*^5(4\lambda_3(x_*-1)^4 + (x_*-3)^2 \times (2x_*+1)) + 2\lambda_1^2(x_*-3)^2(x_*-1)^2x_*^2(6\lambda_3(x_*-1)^4(x_*+2) - (x_*-3)(x_*(x_*(x_*+6)-11)+6)) - 2\lambda_1(x_*-3)(x_*-1)^4 \times x_*^3\left(4\lambda_3(3x_*+2)(x_*-1)^4 + (x_*-3)(x_*(x_*(2x_*-13)+5)-6)\right)\},$$

$$\bar{c}_{12} = \frac{2(x_*-1)^2x_* - \lambda_1(x_*-3)}{(x_*-3)x_*^2}\left\{\frac{2(x_*-3)x_*}{(2(x_*-1)^2x_* - \lambda_1(x_*-3))^3}(2(x_*-1)^3 \times x_*^2 - \lambda_1(x_*-3)(x_*-2)(x_*+1)) - \frac{2(x_*-1)^2x_* - \lambda_1(x_*-3)}{\left(\lambda_1(x_*-3) - 2(x_*-1)^2x_*\right)^2} \times \left(2(x_*-1)x_*^2 - \lambda_1(x_*-3)\right)\left(\frac{(x_*-3)\left(2(x_*-1)x_*^2 - \lambda_1(x_*-3)\right)}{\left(\lambda_1(x_*-3) - 2(x_*-1)^2x_*\right)^2} - \frac{\lambda_3 - \frac{x_*-3}{2(x_*-1)^2}}{x_*}\right) + \frac{\lambda_3 - \frac{x_*-3}{2(x_*-1)^2}}{x_*}\right\},$$

$$\bar{c}_{40} = \frac{1}{2(x_*-3)(x_*-1)^2x_*^3(2(x_*-1)^2x_* - \lambda_1(x_*-3))^5}\{2\lambda_1^6(x_*-3)^6 \times (x_*-1)\left(-2\lambda_3(x_*-1)^2 + x_* - 3\right) + 4\lambda_1^3(x_*-3)^3(x_*-1)^4x_*^2 \times (x_*(x_*(7(x_*-2)x_*+26)+7)-8)\left(2\lambda_3(x_*-1)^2 - x_* + 3\right) - \lambda_1^4$$

$$\times(x_*-3)^4(x_*-1)^2x_*\left(x_*^2(13x_*(3x_*-8)+101)-12\right)$$
$$\times\left(2\lambda_3(x_*-1)^2-x_*+3\right)+\lambda_1^5(x_*-3)^5(x_*(x_*(x_*(15x_*-43)$$
$$+42)-10)-2)\left(2\lambda_3(x_*-1)^2-x_*+3\right)+16(x_*-1)^9x_*^6$$
$$\times(-\lambda_2\left(((x_*-5)x_*+5)x_*^2+x_*+6\right)-2(x_*-3)^2x_*^2(x_*-1)$$
$$+2\lambda_3(x_*(x_*(3x_*-8)-1)-2)(x_*-1)^3)+4\lambda_1^2(x_*-3)^2(x_*-1)^5$$
$$\times x_*^3\left(4\lambda_3\left(x_*\left(x_*\left(6x_*^2-20x_*-9\right)+5\right)+2\right)(x_*-1)^3+(x_*-3)\right.$$
$$\times(-\lambda_2(x_*-3)x_*\left(x_*^2+x_*-4\right)-x_*(x_*(x_*(x_*(11x_*-49)+27)+9)$$
$$+6)+4))+16\lambda_1(x_*-3)(x_*-1)^7x_*^4\left(5(x_*-3)^2x_*^3(x_*-1)-2\lambda_3\right.$$
$$\times(x_*(x_*(x_*(6x_*-17)-4)+5)-2)(x_*-1)^3+\lambda_2(x_*-3)$$
$$\times((x_*-1)x_*((x_*-1)x_*-5)-2))\},$$

$$\bar{c}_{31}=\frac{1}{(x_*-3)(x_*-1)^2x_*^3\left(2(x_*-1)^2x_*-\lambda_1(x_*-3)\right)^5}\{\lambda_1^6(x_*-3)^6$$
$$\times\left(-2\lambda_3(x_*-1)^2+x_*-3\right)+\lambda_1^5(x_*-3)^5x_*(x_*(10x_*-19)+11)$$
$$\times\left(2\lambda_3(x_*-1)^2-x_*+3\right)+16(x_*-1)^9x_*^6(3(x_*-3)\left((x_*-2)x_*^2-1\right)$$
$$-4\lambda_3(x_*-1)^3(x_*+1))+4\lambda_1^2(x_*-3)^2(x_*-1)^5x_*^3((x_*-3)(x_*(x_*$$
$$\times(x_*(31x_*-80)+86)-47)+6)-40\lambda_3(x_*-1)^3x_*((x_*-1)x_*+2))$$
$$+8\lambda_1(x_*-3)(x_*-1)^7x_*^4(4\lambda_3(x_*-1)^3x_*\left(2x_*^2+x_*+7\right)-(x_*-3)$$
$$\times(x_*(x_*(x_*(13x_*-30)+16)-5)-2))+2\lambda_1^3(x_*-3)^3(x_*-1)^3x_*^3$$
$$\times(40\lambda_3(x_*-1)^3(x_*(2x_*-3)+3)-(x_*-3)(x_*(x_*(47x_*-128)$$
$$+148)-77))+2\lambda_1^4(x_*-3)^4(x_*-1)^2x_*^2((x_*-3)(x_*(21x_*-38)+25)$$
$$-10\lambda_3(x_*-1)^2(x_*(4x_*-7)+5))\},$$

$$\bar{c}_{22}=\frac{(3-x_*)\left(2(x_*-1)^2x_*-\lambda_1(x_*-3)\right)^3}{2(x_*-3)^2(x_*-1)^2x_*^4\left(\lambda_1(x_*-3)-2(x_*-1)^2x_*\right)^6}\{3\lambda_1^4(x_*-3)^4$$
$$\times\left(2\lambda_3(x_*-1)^2-x_*+3\right)+8(x_*-1)^5x_*^4(2\lambda_3(x_*-1)^3(5(x_*-1)x_*$$
$$+2)-(x_*-3)(x_*(x_*(7x_*-13)+4)-2))+12\lambda_1(x_*-3)(x_*-1)^3$$
$$\times x_*^3((x_*-3)(x_*(3x_*(3x_*-7)+16)-6)-2\lambda_3(x_*-1)^3(x_*(7x_*-9)$$
$$+4))+6\lambda_1^2(x_*-3)^2(x_*-1)^2x_*^2(2\lambda_3(x_*-1)^2(x_*(11x_*-17)+8)$$
$$-(x_*-3)(x_*(13x_*-21)+10))+\lambda_1^3(x_*-3)^3((x_*-3)x_*(5x_*$$
$$\times(5x_*-9)+22)-2\lambda_3(x_*-1)^2x_*(x_*(23x_*-41)+20))\}.$$

Notice that $\bar{c}_{00}=\bar{c}_{10}=\bar{c}_{01}=\bar{c}_{11}=0$ and system (34) can be simplified as system (22) when $\lambda=0$.

In what follows, we take transformations similar to the seven steps in Li et al.[46] to transform system (34) to system (31).

(I) Eliminating the y^2-term from system (34) when $\lambda=0$. Using $x=X+\frac{\bar{c}_{02}X^2}{2}, y=Y+\bar{c}_{02}XY$, we have

$$\begin{aligned}\frac{dx}{dt}&=y,\\ \frac{dy}{dt}&=\bar{d}_{00}+\bar{d}_{10}x+\bar{d}_{01}y+\bar{d}_{20}x^2+\bar{d}_{11}xy+\bar{d}_{30}x^3+\bar{d}_{21}x^2y+\bar{d}_{12}xy^2+\bar{d}_{40}x^4\\ &\quad+\bar{d}_{31}x^3y+\bar{d}_{22}x^2y^2+o(|x,y|^4),\end{aligned}\tag{35}$$

in which

$$\begin{aligned}&\bar{d}_{00}=\bar{c}_{00},\ \bar{d}_{10}=\bar{c}_{10}-\bar{c}_{00}\bar{c}_{02},\ \bar{d}_{01}=\bar{c}_{01},\ \bar{d}_{20}=\bar{c}_{20}+\bar{c}_{00}\bar{c}_{02}^2-\frac{\bar{c}_{10}\bar{c}_{02}}{2},\\ &\bar{d}_{11}=\bar{c}_{11},\ \bar{d}_{30}=\bar{c}_{30}+\frac{1}{2}(\bar{c}_{10}-2\bar{c}_{00}\bar{c}_{02})\bar{c}_{02}^2,\ \bar{d}_{21}=\bar{c}_{21}+\frac{\bar{c}_{02}\bar{c}_{11}}{2},\\ &\bar{d}_{12}=\bar{c}_{12}+2\bar{c}_{02}^2,\ \bar{d}_{40}=\bar{c}_{40}+\bar{c}_{00}\bar{c}_{02}^4+\frac{1}{4}\big(\bar{c}_{02}(\bar{c}_{20}-2\bar{c}_{02}\bar{c}_{10})+2\bar{c}_{30}\big)\bar{c}_{02},\\ &\bar{d}_{31}=\bar{c}_{31}+\bar{c}_{02}\bar{c}_{21},\ \bar{d}_{22}=\bar{c}_{22}-\bar{c}_{02}^3+\frac{3\bar{c}_{12}\bar{c}_{02}}{2}.\end{aligned}$$

It is worth mentioning that $\bar{d}_{00}=\bar{d}_{10}=\bar{d}_{01}=\bar{d}_{11}=0$ when $\lambda=0$.

(II) Taking xy^2-term away from system (35) when $\lambda=0$. Using the scalings of coordinates $x=X+\frac{\bar{d}_{12}}{6}X^3, y=Y+\frac{\bar{d}_{12}}{2}X^2Y$, we have

$$\begin{aligned}\frac{dx}{dt}&=y,\\ \frac{dy}{dt}&=\bar{e}_{00}+\bar{e}_{10}x+\bar{e}_{01}y+\bar{e}_{20}x^2+\bar{e}_{11}xy+\bar{e}_{30}x^3+\bar{e}_{21}x^2y+\bar{e}_{40}x^4\\ &\quad+\bar{e}_{31}x^3y+\bar{e}_{22}x^2y^2+o(|x,y|^4),\end{aligned}\tag{36}$$

in which

$$\begin{aligned}&\bar{e}_{00}=\bar{d}_{00},\ \bar{e}_{10}=\bar{d}_{10},\ \bar{e}_{01}=\bar{d}_{01},\ \bar{e}_{20}=\bar{d}_{20}-\frac{\bar{d}_{00}\bar{d}_{12}}{2},\ \bar{e}_{11}=\bar{d}_{11},\\ &\bar{e}_{30}=\bar{d}_{30}-\frac{\bar{d}_{10}\bar{d}_{12}}{3},\ \bar{e}_{21}=\bar{d}_{21},\ \bar{e}_{40}=\bar{d}_{40}+\frac{\bar{d}_{00}\bar{d}_{12}^2}{4}-\frac{\bar{d}_{12}\bar{d}_{20}}{6},\\ &\bar{e}_{31}=\bar{d}_{31}+\frac{\bar{d}_{11}\bar{d}_{12}}{6},\ \bar{e}_{22}=\bar{d}_{22}.\end{aligned}$$

We have that $\bar{e}_{00} = \bar{e}_{10} = \bar{e}_{01} = \bar{e}_{11} = 0$ when $\lambda = 0$.

(III) Removing the x^2y^2-term in system (36) when $\lambda = 0$. Setting $x = X + \frac{\bar{e}_{22}}{12}X^4, y = Y + \frac{\bar{e}_{22}}{3}X^3Y$, system (36) can be expressed by

$$\begin{aligned}\frac{dx}{dt} &= y,\\ \frac{dy}{dt} &= \bar{f}_{00} + \bar{f}_{10}x + \bar{f}_{01}y + \bar{f}_{20}x^2 + \bar{f}_{11}xy + \bar{f}_{30}x^3 + \bar{f}_{21}x^2y\\ &\quad + \bar{f}_{40}x^4 + \bar{f}_{31}x^3y + o(|x,y|^4),\end{aligned} \tag{37}$$

in which

$$\bar{f}_{00} = \bar{e}_{00},\ \bar{f}_{10} = \bar{e}_{10},\ \bar{f}_{01} = \bar{e}_{01},\ \bar{f}_{20} = \bar{e}_{20},\ \bar{f}_{11} = \bar{e}_{11},$$
$$\bar{f}_{30} = \bar{e}_{30} - \frac{\bar{e}_{00}\bar{e}_{22}}{3},\ \bar{f}_{21} = \bar{e}_{21},\ \bar{f}_{40} = \bar{e}_{40} - \frac{\bar{e}_{10}\bar{e}_{22}}{4},\ \bar{f}_{31} = \bar{e}_{31}.$$

Again, $\bar{f}_{00} = \bar{f}_{10} = \bar{f}_{01} = \bar{f}_{11} = 0$ when $\lambda = 0$.

(IV) Removing the x^3 and x^4-term in system (37) when $\lambda = 0$. Notice that $\bar{f}_{20} = \frac{1}{2}(1 - x_*) + O(\lambda), \bar{f}_{20} \neq 0$ for small λ since $0 < x_* < \frac{1}{2}$. Making the following scalings $x = X - \frac{\bar{f}_{30}}{4\bar{f}_{20}}X^2 + \frac{15\bar{f}_{30}^2 - 16\bar{f}_{20}\bar{f}_{40}}{80\bar{f}_{20}^2}X^3, y = Y, dt = (1 - \frac{\bar{f}_{30}}{2\bar{f}_{20}}X + \frac{45\bar{f}_{30}^2 - 48\bar{f}_{20}\bar{f}_{40}}{80\bar{f}_{20}^2}X^2)d\tau$, we have

$$\begin{aligned}\frac{dx}{dt} &= y,\\ \frac{dy}{dt} &= \bar{g}_{00} + \bar{g}_{10}x + \bar{g}_{01}y + \bar{g}_{20}x^2 + \bar{g}_{11}xy + \bar{g}_{30}x^3 + \bar{g}_{21}x^2y + \bar{g}_{40}x^4\\ &\quad + \bar{g}_{31}x^3y + o(|x,y|^4),\end{aligned} \tag{38}$$

where

$$\bar{g}_{00} = \bar{f}_{00},\ \bar{g}_{10} = \bar{f}_{10} - \frac{\bar{f}_{00}\bar{f}_{30}}{2\bar{f}_{20}},\ \bar{g}_{01} = \bar{f}_{01},$$
$$\bar{g}_{20} = \bar{f}_{20} + \frac{9\bar{f}_{00}\bar{f}_{30}^2}{16\bar{f}_{20}^2} - \frac{3\left(5\bar{f}_{10}\bar{f}_{30} + 4\bar{f}_{00}\bar{f}_{40}\right)}{20\bar{f}_{20}},$$
$$\bar{g}_{11} = \bar{f}_{11} - \frac{\bar{f}_{01}\bar{f}_{30}}{2\bar{f}_{20}},\ \bar{g}_{30} = \frac{\bar{f}_{10}(35\bar{f}_{30}^2 - 32\bar{f}_{20}\bar{f}_{40})}{40\bar{f}_{20}^2},$$
$$\bar{g}_{21} = \bar{f}_{21} - \frac{3\left(20\bar{f}_{11}\bar{f}_{20}\bar{f}_{30} + \bar{f}_{01}\left(16\bar{f}_{20}\bar{f}_{40} - 15\bar{f}_{30}^2\right)\right)}{80\bar{f}_{20}^2},$$

$$\overline{g}_{40} = \frac{\overline{f}_{10}\overline{f}_{30}(16\overline{f}_{20}\overline{f}_{40} - 15\overline{f}_{30}^{2})}{64\overline{f}_{20}^{3}},$$

$$\overline{g}_{31} = \overline{f}_{31} + \frac{7\overline{f}_{11}\overline{f}_{30}^{2}}{8\overline{f}_{20}^{2}} - \frac{5\overline{f}_{21}\overline{f}_{30} + 4\overline{f}_{11}\overline{f}_{40}}{5\overline{f}_{20}}.$$

Again, $\overline{g}_{00} = \overline{g}_{10} = \overline{g}_{01} = \overline{g}_{11} = \overline{g}_{30} = \overline{g}_{40} = 0$ when $\lambda = 0$.

(V) Taking the x^2y-term away from system (38) when $\lambda = 0$. Observing that $\overline{g}_{20} = \frac{1}{2}(1 - x_*) + O(\lambda)$, $\overline{g}_{20} \neq 0$ for small λ since $0 < x_* < \frac{1}{2}$ and letting

$$x = X, y = Y + \frac{\overline{g}_{21}}{3\overline{g}_{20}}Y^2 + \frac{\overline{g}_{21}^{2}}{36\overline{g}_{20}^{2}}Y^3, d\tau = \left(1 + \frac{\overline{g}_{21}}{3\overline{g}_{20}}Y + \frac{\overline{g}_{21}^{2}}{36\overline{g}_{20}^{2}}Y^2\right)dt,$$

we can rewrite system (38) as

$$\begin{aligned}\frac{dx}{dt} &= y,\\ \frac{dy}{dt} &= \overline{h}_{00} + \overline{h}_{10}x + \overline{h}_{01}y + \overline{h}_{20}x^2 + \overline{h}_{11}xy + \overline{h}_{31}x^3y + \overline{M}_1(x, y, \lambda),\end{aligned} \tag{39}$$

in which

$$\overline{h}_{00} = \overline{g}_{00},\ \overline{h}_{10} = \overline{g}_{10},\ \overline{h}_{01} = \overline{g}_{01} - \frac{\overline{g}_{00}\overline{g}_{21}}{\overline{g}_{20}},$$

$$\overline{h}_{20} = \overline{g}_{20},\ \overline{h}_{11} = \overline{g}_{11} - \frac{\overline{g}_{10}\overline{g}_{21}}{\overline{g}_{20}},\ \overline{h}_{31} = \overline{g}_{31} - \frac{\overline{g}_{21}\overline{g}_{30}}{\overline{g}_{20}}.$$

Here $\overline{h}_{00} = \overline{h}_{10} = \overline{h}_{01} = \overline{h}_{11} = 0$ when $\lambda = 0$, and $\overline{M}_1(x, y, \lambda)$ has the property of (32).

(VI) Changing $\overline{h}_{20}$ and $\overline{h}_{31}$ to 1 in system (39). Direct computation shows that $\overline{h}_{20} = \frac{1-x_*}{2} + O(\lambda) > 0$, $\overline{h}_{31} = \frac{3x_*^3 - 7x_*^2 + 3x_* - 11}{2(x_* - 1)^4 x_*} + O(\lambda) < 0$ for small λ because of $0 < x_* < \frac{1}{2}$. Using the following transformation:

$$x = \overline{h}_{20}^{\frac{1}{5}}\overline{h}_{31}^{-\frac{2}{5}}X,\ \ y = \overline{h}_{20}^{\frac{4}{5}}\overline{h}_{31}^{-\frac{3}{5}}Y,\ \ t = \overline{h}_{20}^{-\frac{3}{5}}\overline{h}_{31}^{\frac{1}{5}}\tau,$$

system (39) continues as

$$\begin{aligned}\frac{dx}{dt} &= y,\\ \frac{dy}{dt} &= \overline{k}_{00} + \overline{k}_{10}x + \overline{k}_{01}y + x^2 + \overline{k}_{11}xy + x^3y + \overline{M}_2(x, y, \lambda),\end{aligned} \tag{40}$$

in which

$$\overline{k}_{00} = \overline{h}_{00}\overline{h}_{31}^{\frac{4}{5}}\overline{h}_{20}^{-\frac{7}{5}},\ \overline{k}_{10} = \overline{h}_{10}\overline{h}_{31}^{\frac{2}{5}}\overline{h}_{20}^{-\frac{6}{5}},$$
$$\overline{k}_{01} = \overline{h}_{01}\overline{h}_{31}^{\frac{1}{5}}\overline{h}_{20}^{-\frac{3}{5}},\ \overline{k}_{11} = \overline{h}_{11}\overline{h}_{31}^{-\frac{1}{5}}\overline{h}_{20}^{-\frac{2}{5}}.$$

Here, $\overline{k}_{00} = \overline{k}_{10} = \overline{k}_{01} = \overline{k}_{11} = 0$ when $\lambda = 0$, and $\overline{M}_2(x, y, \lambda)$ has the property of (32).

(VII) Eliminating the $\overline{k}_{10}$-term in system (40). Ultimately, making the following transformations:

$$x = X - \frac{\overline{k}_{10}}{2},\ \ y = Y,$$

we can change (40) to

$$\begin{aligned}\frac{dx}{dt} &= y,\\ \frac{dy}{dt} &= \overline{\nu}_1 + \overline{\nu}_2 y + \overline{\nu}_3 xy + x^2 + x^3 y + \overline{M}_3(x, y, \lambda),\end{aligned} \tag{41}$$

in which

$$\overline{\nu}_1 = \overline{k}_{00} - \frac{1}{4}\overline{k}_{10}^2,\ \overline{\nu}_2 = \overline{k}_{01} - \frac{\overline{k}_{10}^3}{8} - \frac{\overline{k}_{11}\overline{k}_{10}}{2},\ \overline{\nu}_3 = \overline{k}_{11} + \frac{3}{4}\overline{k}_{10}^2.$$

Here, $\overline{\nu}_1 = \overline{\nu}_2 = \overline{\nu}_3 = 0$ when $\lambda = 0$ and $\overline{M}_3(x, y, \lambda)$ has the property of (32). Taking into consideration $0 < x_* < \frac{1}{2}$ and carrying out a direct calculation with the assistance of Mathematica, we have

$$\left|\frac{\partial(\overline{\nu}_1, \overline{\nu}_2, \overline{\nu}_3)}{\partial(\lambda_1, \lambda_2, \lambda_3)}\right|_{\lambda=0} = -\frac{2^{\frac{8}{5}}\left(x_*^2 - 6x_* + 11\right)\left(3x_*^3 - 7x_*^2 + 3x_* - 11\right)^{\frac{4}{5}}}{(1 - x_*)^{\frac{28}{5}} x_*^{\frac{4}{5}}} \neq 0.$$

System (41) is exactly (31). According to the results in Dumortier et al.,[47] Chow et al.,[48] or Li et al.,[46] we can derive that system (41) is the universal unfolding of Bogdanov–Takens singularity (cusp case) of codimension 3. The remanent part $\overline{M}_3(x, y, \lambda)$ satisfying the property of (32) has no influence on the bifurcation phenomena. As (a, δ, β) moves around $(a + \lambda_1, \delta + \lambda_2, \beta + \lambda_3)$, the dynamical behaviors of system (7) in a small neighborhood of the positive equilibrium $E_*(x_*, \frac{2(x_*-1)^3 x_*}{x_*-3})$ are equivalent to system (41) in a small neighborhood of $(0, 0, 0)$ as $(\overline{\nu}_1, \overline{\nu}_2, \overline{\nu}_3)$ moving around $(0, 0, 0)$. This completes the proof. □

For the normal form (41), we can obtain the Hopf bifurcation surface and homoclinic bifurcation surface in the $(\overline{\nu}_1, \overline{\nu}_2, \overline{\nu}_3)$ parameter space by a similar method used for analyzing the codimension 3 Bagdanov–Takens bifurcation in Yu and Zhang.[49] Obviously, the two equilibria

$E_{\pm}$ of (41) are

$$E_{\pm}(\pm\sqrt{-\overline{\nu}_1}, 0), \quad \text{for } \overline{\nu}_1 < 0.$$

The Jacobian matrix of system (41) at $E_{\pm}$ is expressed by

$$J(E_{\pm}) = \begin{bmatrix} 0 & 1 \\ \pm 2\sqrt{-\overline{\nu}_1} & \overline{\nu}_2 \pm \overline{\nu}_3\sqrt{-\overline{\nu}_1} \mp \overline{\nu}_1\sqrt{-\overline{\nu}_1} \end{bmatrix},$$

which suggests that E_+ is a saddle and E_- is focus or node. It is clear that the plane

$$SN = \{(\overline{\nu}_1, \overline{\nu}_2, \overline{\nu}_3) | \overline{\nu}_1 = 0\},$$

excluding the origin in the parameter space is the saddle-node bifurcation surface.

Next, we focus on Hopf bifurcation and generalized Hopf bifurcation from which multiple limit cycles can occur. Following the procedure described in Yu and Zhang,[49] we have the following result.

Theorem 7. *For system (41), Hopf bifurcation occurs from the equilibrium* E_- *at any point on the critical surface defined by*

$$H = \left\{ (\overline{\nu}_1, \overline{\nu}_2, \overline{\nu}_3) | \overline{\nu}_2 - (\overline{\nu}_3 - \overline{\nu}_1)\sqrt{-\overline{\nu}_1} = 0 \right\}.$$

The generalized Hopf bifurcation occurs from the equilibrium E_- *at any point on the critical line, which is the intersection of the critical surface* H *and the generalized critical surface* GH *defined by*

$$GH = \{(\overline{\nu}_1, \overline{\nu}_2, \overline{\nu}_3) | \overline{\nu}_3 - 3\overline{\nu}_1 = 0\}.$$

This yields two small-amplitude limit cycles. The inner limit cycle is stable and the outer is unstable.

Now we are committed to investigating the homoclinic bifurcation surface as well as the degenerate homoclinic bifurcation points on the surface. We have the following theorem.

Theorem 8. *For system (41), the homoclinic bifurcation can occur from the critical surface defined by*

$$HL = \left\{ (\overline{\nu}_1, \overline{\nu}_2, \overline{\nu}_3) | \overline{\nu}_2 - \frac{5}{7}\left(\overline{\nu}_3 - \frac{103}{55}\overline{\nu}_1\right)\sqrt{-\overline{\nu}_1} = 0 \right\}, \tag{42}$$

and the degenerate homoclinic bifurcation occurs from any point on the critical line, which is the intersection of the critical surface HL *and the degenerate critical surface* DHL *defined by*

$$DHL = \{(\overline{\nu}_1, \overline{\nu}_2, \overline{\nu}_3) | \overline{\nu}_2 + (\overline{\nu}_3 - \overline{\nu}_1)\sqrt{-\overline{\nu}_1} = 0\}. \tag{43}$$

This leads to the occurrence of two limit cycles.

3.3 | Degenerate focus-type Bogdannov–Takens bifurcation of codimension 3

According to Theorem 4, system (7) may undergo degenerate focus-type Bogdannov–Takens bifurcation of codimension 3 under appropriate parameters. To this end, we take a, δ, and β as bifurcation parameters and consider the following unfolding system of system (7):

$$\begin{cases} \frac{dx}{dt} = x(1-x) - \frac{xy}{x^2+dx+(a+r_1)}, \\ \frac{dy}{dt} = y(\delta + r_2 - \frac{(\beta+r_3)y}{x}), \end{cases} \tag{44}$$

where $a = \frac{(1-d)^3}{27}$, $\delta = \frac{d+2}{3}$, $\beta = \frac{9}{(d+2)^2}$, $\max\{-2\sqrt{a}, -2\} < d < 1$, and $r = (r_1, r_2, r_3) \sim (0,0,0)$. The following is our main theorem.

Theorem 9. *Suppose that the condition (II) in Theorem 2 is satisfied and $\delta = \frac{d+2}{3}$, then system (7) has a nilpotent focus of codimension 3, $E^*(x^*, \frac{\delta}{\beta}x^*) = (\frac{1-d}{3}, \frac{(1-d)(d+2)^3}{81})$, where $-2 < d < 1$. Furthermore, when parameters (a, β, δ) change in a small neighborhood of $(\frac{(1-d)^3}{27}, \frac{9}{(d+2)^2}, \frac{d+2}{3})$, where $\max\{-2\sqrt{a}, -2\} < d < 1$, system (7) undergoes a degenerate focus-type Bogdanov–Takens bifurcation of codimension 3 in a small neighborhood of E^*. Therefore, with certain parameter values, system (7) admits one or two Hopf bifurcation surfaces, one or two homoclinic bifurcation surfaces, one saddle-node loop bifurcation surface, and one or two saddle node bifurcation surfaces. Thus, system (7) has three hyperbolic positive equilibria, two limit cycles, bistable states (one stable equilibrium and one stable limit cycle or two stable equilibria), or tristability states (two stable equilibria and one stable limit cycle) with appropriate parameter values.*

Proof. Making transformations (i), (ii), (iii) for system (44), which have been presented in the proof of Theorem 4, we derive an equivalent system

$$\begin{cases} \frac{dx}{dt} = y + a_{00}^*(r) + a_{10}^*(r)x + a_{01}^*(r)y + a_{20}^*(r)x^2 + a_{11}^*(r)xy + a_{02}^*(r)y^2 \\ \qquad + a_{30}^*(r)x^3 + a_{21}^*(r)x^2y + a_{12}^*(r)xy^2 + a_{03}^*(r)y^3 + o(|x,y|^3), \\ \frac{dy}{dt} = b_{00}^*(r) + b_{10}^*(r)x + b_{01}^*(r)y + b_{20}^*(r)x^2 + b_{11}^*(r)xy + b_{02}^*(r)y^2 + b_{30}^*(r)x^3 \\ \qquad + b_{21}^*(r)x^2y + b_{12}^*(r)xy^2 + b_{03}^*(r)y^3 + o(|x,y|^3), \end{cases}$$

where $a_{ij}^*(r)$ and $b_{ij}^*(r)$ are smooth functions satisfying $a_{00}^*(0) = a_{10}^*(0) = a_{01}^*(0) = a_{20}^*(0) = a_{11}^*(0) = a_{02}^*(0) = b_{00}^*(0) = b_{10}^*(0) = b_{01}^*(0) = b_{20}^*(0) = b_{02}^*(0) = 0, a_{30}(0)^* = a_{30}^*, a_{21}^*(0) = a_{21}^*, a_{12}^*(0) = a_{12}^*, a_{03}^*(0) = a_{03}^*, b_{11}^*(0) = b_{11}^*, b_{30}^*(0) = b_{30}^*, b_{21}^*(0) = b_{21}^*, b_{12}^*(0) = b_{12}^*, b_{03}^*(0) = b_{03}^*$, and $a_{30}^*, a_{21}^*, a_{12}^*, a_{03}^*, b_{11}^*, b_{30}^*, b_{21}^*, b_{12}^*, b_{03}^*$ are given in system (25).

Using

$$x = X + \frac{b_{12}^*}{6}X^3 + \frac{a_{12}^* + b_{03}^*}{2}X^2Y + a_{03}^*XY^2,$$

$$y = Y + \frac{b_{12}^*}{2}X^2Y + b_{03}^*XY^2,$$

we can simplify the third-order terms when $r = 0$ and get (for convenience, in every subsequent transformation, we rename X, Y, τ as x, y, t, respectively)

$$\begin{cases} \frac{dx}{dt} = y + c_{00}^*(r) + c_{10}^*(r)x + c_{01}^*(r)y + c_{20}^*(r)x^2 + c_{11}^*(r)xy + c_{02}^*(r)y^2 \\ \quad + c_{30}^*(r)x^3 + c_{21}^*(r)x^2y + c_{12}^*(r)xy^2 + c_{03}^*(r)y^3 + o(|x,y|^3), \\ \frac{dy}{dt} = d_{00}^*(r) + d_{10}^*(r)x + d_{01}^*(r)y + d_{20}^*(r)x^2 + d_{11}^*(r)xy + d_{02}^*(r)y^2 \\ \quad + d_{30}^*(r)x^3 + d_{21}^*(r)x^2y + d_{12}^*(r)xy^2 + d_{03}^*(r)y^3 + o(|x,y|^3). \end{cases} \tag{45}$$

Under the following near-identity transformation

$$\begin{aligned} X &= x, \\ Y &= y + c_{00}^*(r) + c_{10}^*(r)x + c_{01}^*(r)y + c_{20}^*(r)x^2 + c_{11}^*(r)xy + c_{02}^*(r)y^2 \\ &\quad + c_{30}^*(r)x^3 + c_{21}^*(r)x^2y + c_{12}^*(r)xy^2 + c_{03}^*(r)y^3 + o(|x,y|^3), \end{aligned}$$

system (45) continues as

$$\begin{cases} \frac{dx}{dt} = y, \\ \frac{dy}{dt} = e_{00}^*(r) + e_{10}^*(r)x + e_{01}^*(r)y + e_{20}^*(r)x^2 + e_{11}^*(r)xy + e_{02}^*(r)y^2 \\ \quad + e_{30}^*(r)x^3 + e_{21}^*(r)x^2y + e_{12}^*(r)xy^2 + e_{03}^*(r)y^3 + o(|x,y|^3), \end{cases} \tag{46}$$

where $e_{ij}^*(r)$ have complicated expressions of $c_{ij}^*(r)$ and $d_{ij}^*(r)$ and are omitted to save space.

Lastly, following the procedure in Xiao and Zhang,[50] system (46) can be expressed by

$$\begin{cases} \frac{dx}{dt} = \frac{\sigma^*(r)}{\nu^*(r)}y, \\ \frac{dy}{dt} = \frac{-e_{30}^*(r)}{\sigma^*(r)}[\lambda_1(r) + \lambda_2(r)\nu^*(r)x - \nu^{*3}x^3] + e_{21}^*(r)y[\lambda_3(r) + A^*(r)\nu^*(r)x \\ \quad + \nu^{*2}(r)x^2] + y^2N_1^*(x,y,r) + o(|x,y|^3), \end{cases}$$

in which

$$\lambda_1(r) = -\frac{e_{00}^*(r)}{e_{30}^*(r)} + \frac{e_{10}^*(r)e_{20}^*(r)}{3e_{30}^{*2}(r)} - \frac{e_{20}^{*3}(r)}{9e_{30}^{*3}(r)} + \frac{e_{20}^{*3}(r)}{27e_{30}^{*3}(r)},$$

$$\lambda_2(r) = -\frac{e_{10}^*(r)}{e_{30}^*(r)} + \frac{e_{20}^{*2}(r)}{3e_{30}^{*2}(r)},$$

$$\lambda_3(r) = -\frac{e_{01}^*(r)}{e_{21}^*(r)} - \frac{e_{11}^*(r)e_{20}^*(r)}{3e_{21}^*e_{30}^*(r)} + \frac{e_{21}^*e_{20}^{*2}(r)}{9e_{21}^*e_{30}^{*2}(r)},$$

$$A(r)=\frac{e_{11}^*(r)}{e_{21}^*(r)}+\frac{2e_{20}^*(r)}{3e_{30}^*(r)},$$

$$N_1^*(x,y,r)=\sigma^*(r)[e_{02}^*(r)+\frac{e_{12}^*(r)e_{20}^{*2}(r)}{9e_{30}^{*2}(r)}+\sigma^*(r)e_{03}^*(r)y+\nu^*(r)e_{12}^*(r)x].$$

By computation with Mathematica, one obtains that $e_{30}^*(0)=-\frac{3}{4(d+2)^7}<0$ and $e_{21}^*(0)=-\frac{3(4-d)(5-2d)}{8(1-d)(d+2)^8}<0$. Thus, we can take

$$\sigma^*(r)=-\frac{e_{30}^*(r)}{e_{21}^*(r)}\nu^*(r),\ \nu^*(r)=\sqrt{-\frac{e_{30}^*(r)}{e_{21}^{*2}(r)}},$$

in the small neighborhood of $r=(0,0,0)$. Eventually, taking a change of time $\tau=-\frac{e_{30}^*(r)}{e_{21}^*(r)}t$, we get

$$\begin{cases}\frac{dx}{dt}=y,\\ \frac{dy}{dt}=\mu_1^*(r)+\mu_2^*(r)x-x^3+y[\mu_3^*(r)+A_1^*(r)x+x^2]+y^2N_2^*(x,y,r)+o(|x,y|^3),\end{cases}\tag{47}$$

in which $A_1^*(r)=\frac{e_{21}^*(r)\sqrt{-e_{30}^*(r)}}{e_{30}^*(r)}A^*(r), N_2^*(x,y,r)=-\frac{e_{21}^*(r)}{e_{30}^*(r)}N_1^*(x,y,r)$, and

$$\mu_1^*(r)=\frac{e_{21}^{*3}(r)}{e_{30}^*(r)\sqrt{-e_{30}^*(r)}}\lambda_1(r),\ \mu_2^*(r)=-\frac{e_{21}^{*2}(r)}{e_{30}^*(r)}\lambda_2(r),\ \mu_3^*(r)=-\frac{e_{21}^{*3}(r)}{e_{30}^*(r)}\lambda_3(r).$$

In view of $\max\{-2\sqrt{a},-2\}<d<1$, tedious calculation leads to

$$\left|\frac{\partial(\mu_1^*(r),\mu_2^*(r),\mu_3^*(r))}{\partial(r_1,r_2,r_3)}\right|_{r=0}\neq 0\ \text{ and }\ A_1^*(0)=\sqrt{\frac{d+2}{3}}<2\sqrt{2}.$$

Based on the results in Refs. [25, 50], we know that system (47) is a standard family of Bogdanov–Takens singularity of codimension 3 (focus case), which indicates that system (7) exhibits a degenerate focus-type Bogdanov–Takens bifurcation of codimension 3 by choosing a,δ, and β as bifurcation parameters in a small neighborhood of $(\frac{(1-d)^3}{27},\frac{9}{(d+2)^2},\frac{d+2}{3})$. □

3.4 | Hopf bifurcation

From the analysis Theorem 3 (I)(i), system (7) may undergo Hopf bifurcation around E_1 (or E_3). This will be studied in detail in this subsection.

Performing the same process as (13) to (17), we obtain that

$$\begin{cases}\frac{dx}{dt}=\frac{1}{m^3}x^2(x^2+dx+a)(m-x)+\frac{(1+d+a)(1-m)}{m^3}x^2y,\\ \frac{dy}{dt}=\delta y(x^2+dx+a)(x-y),\end{cases}\tag{48}$$

where the parameters satisfy that $0 < m < 1, a, \delta > 0, d > -2\sqrt{a}$ and transformation (14) guarantees that the qualitative properties between system (48) and system (7) are the same. For simplicity, we denote

$$\delta_* = \frac{-a + d(m-2) + 2m - 3}{m^3(a + d + 1)} > 0.$$

We have the following theorem.

Theorem 10. *Assume that* $0 < m < 1, a, \delta > 0, d > -2\sqrt{a}$. *Then,* $\widetilde{\mathrm{E}}(1,1)$ *is a equilibrium of system (48). Furthermore, if* $(a-1)m + d + 2 > 0$, *then we have*

(I) when $\delta < \delta_*$, $\widetilde{\mathrm{E}}(1,1)$ *is an unstable hyperbolic node or focus;*
(II) when $\delta > \delta_*$, $\widetilde{\mathrm{E}}(1,1)$ *is a stable hyperbolic node or focus;*
(III) when $\delta = \delta_*$, $\widetilde{\mathrm{E}}(1,1)$ *is a weak focus or center.*

Proof. The Jacobian matrix of system (48) at $\widetilde{\mathrm{E}}(1,1)$ is

$$J(\widetilde{\mathrm{E}}(1,1)) = \begin{pmatrix} \frac{-a+d(m-2)+2m-3}{m^3} & -\frac{(m-1)(a+d+1)}{m^3} \\ \delta(a+d+1) & \delta(-(a+d+1)) \end{pmatrix}.$$

The determinant and the trace of $J(\widetilde{\mathrm{E}}(1,1))$ are

$$\det(J(\widetilde{\mathrm{E}})) = \frac{\delta(a+d+1)((a-1)m+d+2)}{m^3},$$

and

$$\mathrm{tr}(J(\widetilde{\mathrm{E}})) = -\frac{\delta m^3(a+d+1) + a - d(m-2) - 2m + 3}{m^3},$$

respectively. Because of $0 < m < 1, a, \delta > 0, d > -2\sqrt{a}$, and $(a-1)m + d + 2 > 0$, one gets that $\det(J(\widetilde{\mathrm{E}})) > 0$, and $\mathrm{tr}(J(\widetilde{\mathrm{E}})) = 0 (> 0, < 0)$ if $\delta = \delta_* (\delta < \delta_*, \delta > \delta_*)$. We complete the proof. □

In the subsequent work, we focus on the case $\delta = \delta_*$ of Theorem 10. Denoting

$$\sigma_{11} = p_2 m^2 + p_1 m + p_0, \tag{49}$$

where

$$\begin{aligned} p_2 &= 2ad^2 + (a+1)^3 d + 2a\left(3a^2 - 2a + 3\right), \\ p_1 &= -3ad^3 - \left(6a^2 + 15a + 1\right)d^2 - \left(6a^3 + 19a^2 + 24a + 3\right)d \\ &\quad - a\left(a^3 + 15a^2 + 3a + 21\right), \\ p_0 &= d^3 + \left(-a^2 + 3a + 6\right)d^2 + \left(-3a^2 + 14a + 9\right)d + a^3 - 3a^2 + 15a + 3, \end{aligned}$$

we have the following theorems.

Theorem 11. *Suppose that* $0 < m < 1, a, \delta = \delta_* > 0, d > -2\sqrt{a}$, *and* $(a-1)m + d + 2 > 0$. *Then we have*

(*I*) *if* $\sigma_{11} < 0$, *then* $\widetilde{E}(1,1)$ *is a stable weak focus with multiplicity 1 and one stable limit cycle bifurcates from* $\widetilde{E}(1,1)$ *by a supercritical Hopf bifurcation;*
(*II*) *if* $\sigma_{11} > 0$, *then* $\widetilde{E}(1,1)$ *is an unstable weak focus with multiplicity 1 and one unstable limit cycle bifurcates from* $\widetilde{E}(1,1)$ *by a subcritical Hopf bifurcation;*
(*III*) *if* $\sigma_{11} = 0$, *then* $\widetilde{E}(1,1)$ *is a weak focus with multiplicity at least two and system (48) may exhibit a degenerate Hopf bifurcation.*

Proof. Introducing $X = x - 1, Y = y - 1$, and $\delta = \delta_*$ into system (48), we derive an equivalent system to (48) as follows (for convenience, in every subsequent transformation, we rename X, Y, τ as x, y, t, respectively).

$$\begin{aligned}
\frac{dx}{dt} &= \widetilde{b}x - \widetilde{q}y + \frac{-2a + 2dm - 5d + 5m - 9}{m^3}x^2 - \frac{2(m-1)(a+d+1)}{m^3}xy + \\
&\quad \frac{-a + d(m-4) + 4m - 10}{m^3}x^3 - \frac{(m-1)(a+d+1)}{m^3}x^2y + o(|x,y|^3), \\
\frac{dy}{dt} &= \widetilde{b}x - \widetilde{b}y + \frac{(d+2)(-a + d(m-2) + 2m - 3)}{m^3(a+d+1)}x^2 - \frac{a-1}{m^3(a+d+1)} \\
&\quad \times (a - (d+2)m + 2d + 3)xy + \frac{a - (d+2)m + 2d + 3}{m^3}y^2 \\
&\quad + \frac{-a + d(m-2) + 2m - 3}{m^3(a+d+1)}x^3 + \frac{(d+1)(-a + d(m-2) + 2m - 3)}{m^3(a+d+1)}x^2y \\
&\quad + \frac{(d+2)(a - (d+2)m + 2d + 3)}{m^3(a+d+1)}xy^2 + o(|x,y|^3),
\end{aligned} \tag{50}$$

in which $\widetilde{b} = \frac{-a+d(m-2)+2m-3}{m^3} > 0$ on account of $\delta_* > 0$ and $\widetilde{q} = \frac{(m-1)(a+d+1)}{m^3}$.

Let $\omega = \sqrt{\widetilde{b}\widetilde{q} - \widetilde{b}^2}$ and

$$x = \widetilde{q}X,\ y = \widetilde{b}X - \omega Y,\ dt = \frac{1}{\omega}d\tau. \tag{51}$$

It follows from (50) that

$$\begin{aligned}
\frac{dx}{dt} &= y + u(x,y), \\
\frac{dy}{dt} &= -x + v(x,y),
\end{aligned}$$

in which

$$\begin{aligned}
u(x,y) &= u_{20}x^2 + u_{11}xy + u_{30}x^3 + u_{21}x^2y + o(|x,y|^3), \\
v(x,y) &= v_{20}x^2 + v_{11}xy + v_{02}y^2 + v_{30}x^3 + v_{21}x^2y + v_{12}xy^2 + o(|x,y|^3),
\end{aligned}$$

and

$$u_{20} = -\frac{(m-1)(a+d+1)(d-m+3)}{m^3\sqrt{(-a+d(m-2)+2m-3)((a-1)m+d+2)}},$$

$$u_{11} = \frac{2(m-1)(a+d+1)}{m^3},$$

$$u_{30} = -\frac{(m-1)^2(a+d+1)^2(2d-2m+7)}{m^6\sqrt{(-a+d(m-2)+2m-3)((a-1)m+d+2)}},$$

$$u_{21} = \frac{(m-1)^2(a+d+1)^2}{m^6},$$

$$\begin{aligned} v_{20} = {} & \frac{1}{m^3((a-1)m+d+2)}\{m\left(a^2+2(a-8)d-3d^2-17\right)+2ad+5a \\ & +m^2(-a(2d+3)+3d+5)+4d^2+15d+13\}, \end{aligned}$$

$$v_{11} = \frac{1}{m^3}\sqrt{\frac{-a+d(m-2)+2m-3}{(a-1)m+d+2}}(3(a-1)m-a+2d+5),$$

$$v_{02} = \frac{-a+d(m-2)+2m-3}{m^3},$$

$$\begin{aligned} v_{30} = {} & \frac{m-1}{m^6((a-1)m+d+2)}\{21+d(d(4d+23)+39)-26m+(3d(d+3) \\ & +7)m^2-d(d(3d+22)+43)m+a^2\left(-(d+6)m+2d+m^2+7\right) \\ & +a\left(d\left(-(d+1)m^2-2(d+8)m+5d+23\right)-16m+20\right)\}, \end{aligned}$$

$$\begin{aligned} v_{21} = {} & \frac{m-1}{m^6}\sqrt{\frac{-a+d(m-2)+2m-3}{(a-1)m+d+2}}\{a^2(m-1)+3a(d+1)m-ad \\ & +a+2d(d-2m+5)-6m+10\}, \end{aligned}$$

$$v_{12} = \frac{(d+2)(m-1)(-a+d(m-2)+2m-3)}{m^6}.$$

In accordance with the formula in Perko[40] and by Mathematica, the first Lyapunov coefficient can be calculated by

$$\sigma_1 = \frac{(m-1)^2\sigma_{11}}{8m^6((a-1)m+d+2)\sqrt{(-a+d(m-2)+2m-3)((a-1)m+d+2)}},$$

where σ_{11} is expressed in (49). In view of $(a-1)m+d+2>0$, the sign of σ_1 is determined by σ_{11} and thus the proof is finished. □

Following we further study the case (III) in Theorem 11 to determine the exact codimension of Hopf Bifurcation around $\widetilde{E}(1,1)$. A complicated calculation with the assistant of Maple and

Mathematica yields the second Lyapunov coefficients as follows:

$$\sigma_2 = \frac{\sqrt{(-a + d(m-2) + 2m - 3)((a-1)m + d + 2)}}{288m^{12}((a-1)m + d + 2)^4(a - (d+2)m + 2d + 3)^2}\sigma_{22},$$

where σ_{22} is given in the Appendix, then we have the following:

Theorem 12. *Suppose that* $0 < m < 1, a, \delta = \delta_* > 0, d > -2\sqrt{a}$, *and* $(a-1)m + d + 2 > 0$ *and* $\sigma_{11} = 0$, *then*

(*I*) *if* $\sigma_{22} < 0$, *then* $\tilde{E}(1,1)$ *is a stable weak focus with multiplicity 2, system (48) undergoes a degenerate Hopf bifurcation of codimension 2 and there can be up to two limit cycles bifurcating from* $\tilde{E}$, *the outer one being stable;*

(*II*) *if* $\sigma_{22} > 0$, *then* $\tilde{E}(1,1)$ *is an unstable weak focus with multiplicity 2, model (48) undergoes a degenerate Hopf bifurcation of codimension 2 and there can be up to two limit cycles bifurcating from* $\tilde{E}$, *the outer one being unstable;*

(*III*) *if* $\sigma_{22} = 0$, *then* $\tilde{E}(1,1)$ *is a weak focus with multiplicity at least 3 and model (48) may undergo a degenerate Hopf bifurcation of codimension at least 3.*

4 | NUMERICAL ANALYSIS

In this section, we give some numerical simulations and phase portraits for system (7) by using the ODE packages in AUTO07P.[51] The main objective of this section is to illustrate the complex dynamics under some primary parameters. We select the following set of parameters value for system (7): $a = 0.03, \delta = 0.5515528128088303, \beta = 1.9107764064044153, d = 0.05$.

4.1 | β as the primary bifurcation parameter

First, β is used as the primary bifurcation parameter. We have two subcritical Hopf bifurcation points: $HB_1(1.36947 \times 10^{-1}, 4.79873 \times 10^{-2})$ when $\beta = 1.57403$, and $HB_2(4.10619 \times 10^{-1}, 1.29156 \times 10^{-1})$ when $\beta = 1.75352$. The first Lyapunov coefficients of HB_1 and HB_2 are, respectively, 1.020204×10^1 and 8.618838; two saddle-node bifurcation points: $S\bar{N}_1(3.57894 \times 10^{-1}, 1.13000 \times 10^{-1})$ when $\beta = 1.74689$, $S\bar{N}_2(2.71488 \times 10^{-1}, 8.54400 \times 10^{-2})$ when $\beta = 1.75257$. If we continue one-parameter periodic orbit bifurcation curve, then we have two saddle-node bifurcation points $SN_1(4.01146 \times 10^{-1}, 1.35392 \times 10^{-1})$ with $\beta = 1.51324$, period $= 1.90645 \times 10^1$, and $SN_2(4.10647 \times 10^{-1}, 1.29165 \times 10^{-1})$ with $\beta = 1.76613$, period $= 4.34988 \times 10^1$, respectively. The results are shown in Figure 4A,B, where the solid curve and the dotted curve represent the stable and unstable equilibrium or limit cycle, respectively.

Within the context of an outbreak modeled by a system with multiple stable solutions, a characteristic is commonly referred to as metastability in Wollkind et al.[12] or subcritical instability, with one such solution characterized by a low prey level and another by a high prey level. Outbreaks are induced either by changing a control parameter or by perturbing the population so that the populations move from the basin of attraction of low level solution through a threshold into the basin of attraction of the high level solution. The stable states are the two positive equilibrium points separated by a saddle point.

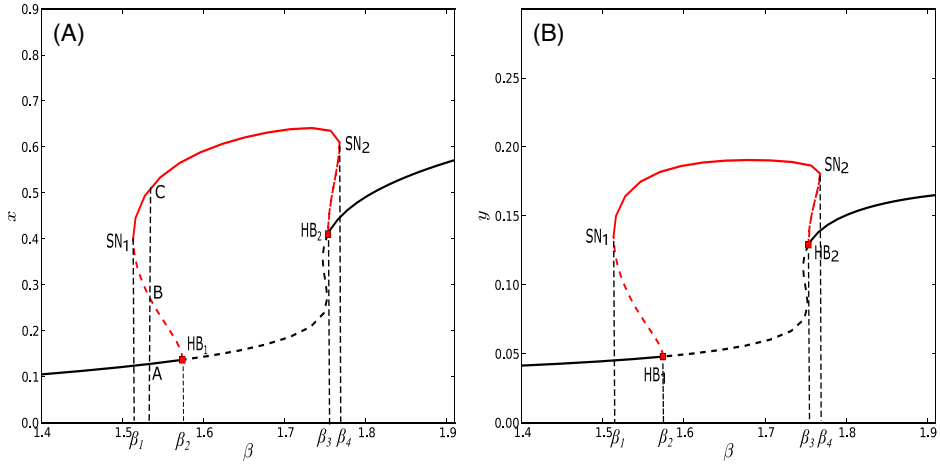

FIGURE 4 One-parameter bifurcation diagram of system (7) for β, where HB_1 and HB_2 denote the subcritical Hopf bifurcation points, SN_1 and SN_2 denote the saddle-node bifurcation point (red) of limit cycle.

We now consider the implications of the bifurcation diagram in Figure 4A,B with respect to the global behavior of system (7). Four important values of β are indicated on the horizontal axis. The first two are the values β_2 and β_3 for the occurrence of Hopf bifurcation as described above, and the remaining two are $\beta_1 = 1.511324$ and $\beta_4 = 1.76613$ for the occurrence of saddle-node bifurcation point of limit cycle as the parameter values vary. The lowest value for which there is a periodic solution corresponds to the limit point mentioned above. These four values divide the interval into five subintervals. Within each subinterval, the system possesses the same qualitative global behavior. We note that, for this reason, Figure 4 only shows those values of β given by $1.4 < \beta < 1.92$. For $\beta < \beta_1$ and $\beta > \beta_4$, the behavior is qualitatively equivalent to that for $1.4 < \beta < \beta_1$ and $\beta_4 < \beta < 1.92$, respectively.

Given any fixed value of β, the global behavior of system (7) can be deduced by examining the intersection of the bifurcation diagram with a vertical line through that value of β. Thus, we must consider all branches of the diagram above with the value of β under consideration. We can make the following conclusions concerning the global behavior. For $0 < \beta < \beta_1$, system (7) possesses a globally stable equilibrium point exhibiting low population levels. For $\beta > \beta_4$ the system possesses a globally stable equilibrium point exhibiting relatively high population levels. For $\beta_1 < \beta < \beta_4$, the system possesses an unstable equilibrium point surrounded in the phase plane by a globally stable limit cycle. The amplitude of the prey oscillations increases as β increases, as shown in Figure 4A.

Since the dynamics between β_1 and β_2 are similar to that between β_3 and β_4, we only need to consider the behavior exhibited by system (7) in the interval $\beta_1 < \beta < \beta_2$. Referring to the vertical line in Figure 4 at $\beta_1 = 1.511324$, the point labeled A corresponds to a stable fixed point, while B corresponds to an unstable small limit cycle and C corresponds to a stable large limit cycle. Thus, for β in this interval, system (7) has multiple solutions consisting of a stable equilibrium point surrounded in the phase plane by an unstable limit cycle, which in turn is surrounded by a stable large limit cycle, with the unstable small limit cycle acting as the separatrix between the basin of attraction of the equilibrium point and that of the stable limit cycle. Thus, populations lying inside the unstable limit cycle will tend to the fixed point while populations outside this region will tend to the stable limit cycle.

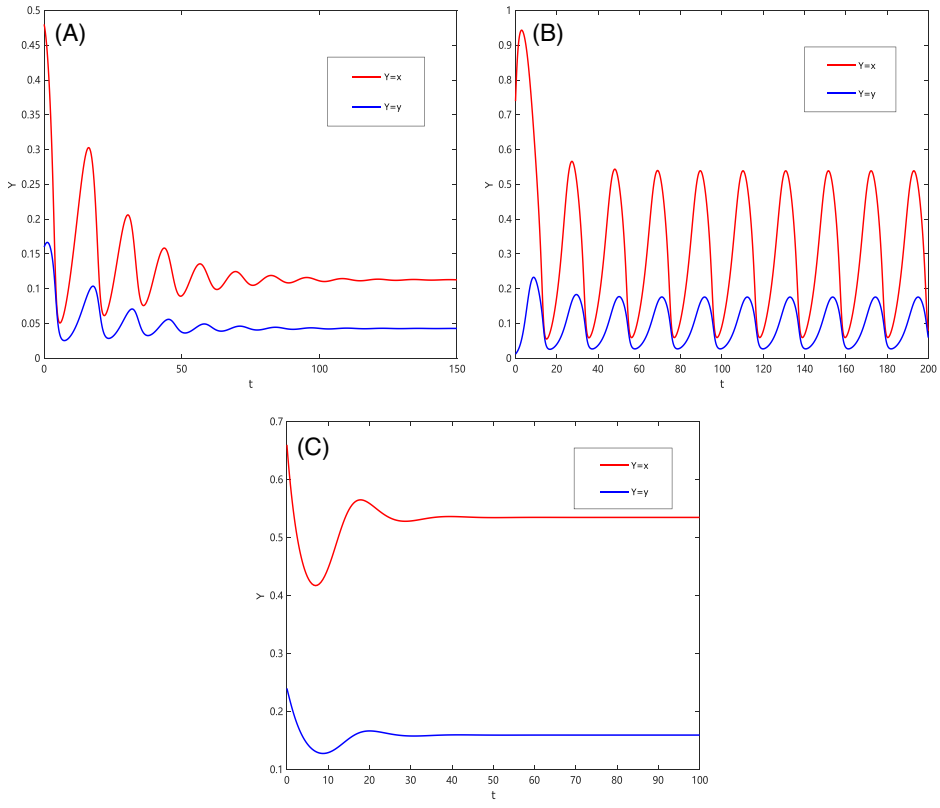

FIGURE 5 Plots of the dimensional variables x and y illustrate population densities at (A) $\beta = 1.45$, the initial value is (0.48,0.16); (B) $\beta = 1.55$, the initial value is (0.739365,0.012422); (C) $\beta = 1.85$, the initial value is (0.66,0.24).

We find that the consequence of this interval of metastability is due to the presence of hysteresis behavior as β varies. If we assume populations are initially at a steady-state solution and only vary the parameter β, the behavior exhibited for $\beta_1 < \beta < \beta_2$ will depend on where β is initially. When β is initially less than β_1 and increases to fall in the interval (β_1, β_2), the populations will start at a globally stable equilibrium point and remain until β exceeds β_2, at which the system will spontaneously jump to the branch of stable oscillations causing the populations to spiral out to the limit cycle. When β is initially greater than β_2 and decreases, populations will initially be oscillating as determined by the globally stable limit cycle. As β decreases to below β_2 (into the interval of metastability), these populations will be within the basin of attraction of the limit cycle and continue to oscillate until β decreases below β_1, at which the system will spontaneously jump to the branch of stable fixed point solutions causing the oscillations to diminish as the populations spiral in toward the fixed point. As will be discussed below, both the metastability and hysteresis behavior may result in a population outbreak. Thus, if the population undergoing an outbreak is a pest species, the economical and ecological consequence can be severe. We can make the following conclusions concerning the global behavior. For $0 < \beta < \beta_1$, system (7) possesses a globally stable equilibrium exhibiting a relatively low level. For $\beta > \beta_4$, the system possesses a globally stable equilibrium exhibiting a relatively high level. See the results with $\beta = 1.45$ in Figure 5A, and with

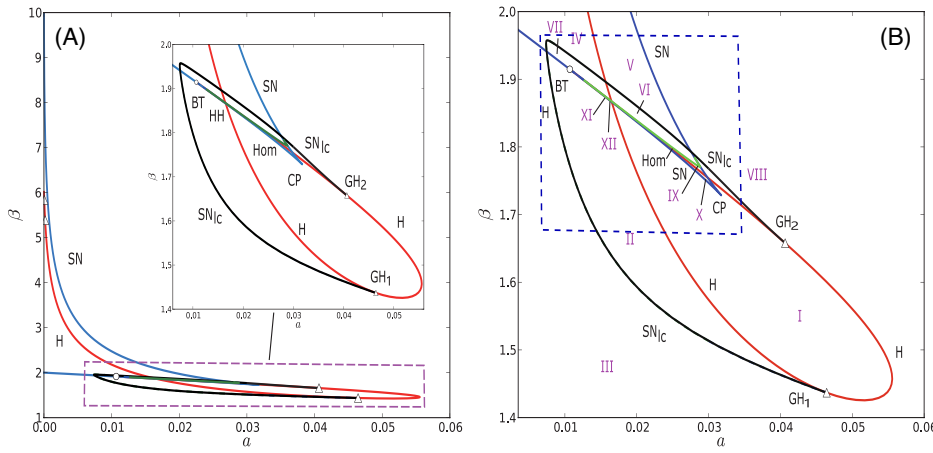

FIGURE 6 Two-parameter bifurcation diagram with β vs. a of system (7) where SN, H, Hom, SN_{lc} denote the saddle-node bifurcation curve (blue), Hopf bifurcation curve (red), homclinic bifurcation curve (green), and saddle-node curve (black) of limit cycles, respectively. (A) The whole bifurcation diagram for β vs. a. (B) The first zoomed bifurcation diagram and 12 regions for β vs. a.

$\beta = 1.55$ in Figure 5B. For $\beta_1 < \beta < \beta_2$, the system possesses an unstable equilibrium surrounded by a globally stable limit cycle.

4.2 | a and β as the primary bifurcation parameters

In this subsection, we use a and β as the primary bifurcation parameters. Then, we obtain two-parameter bifurcation diagrams including Hopf bifurcation curve (red), saddle-node bifurcation curve (blue), homoclinic bifurcation curve (green), and saddle-node bifurcation curve (black) of limit cycles. There are one codimension 2 Bagdanov–Takens bifurcation point $BT(4.48447 \times 10^{-1}, 1.29178 \times 10^{-1})$ as $\beta = 1.06798 \times 10^{-2}, a = 1.91475$, one codimension 2 cusp bifurcation point $CP(3.16667 \times 10^{-1}, 1.01042 \times 10^{-1})$ as $\beta = 3.17546 \times 10^{-2}, a = 1.72858$, two generalized Hopf bifurcation points: $GH_1(3.82518 \times 10^{-1}, 1.27262 \times 10^{-1})$ as $\beta = 4.06517 \times 10^{-2}, a = 1.65784$, $GH_2(2.03103 \times 10^{1}, 7.79707 \times 10^{-2})$ as $\beta = 4.64371 \times 10^{-2}, a = 1.43672$. The second Lyapunov coefficients of GH_1 and GH_2 are, respectively, -2.199578×10^{2} and -4.465886×10^{2}; Interestingly, there is only one global saddle-node bifurcation curve of limit cycle, which is connecting the two generalized Hopf bifurcation points GH_1 and GH_2, rather than distinct saddle-node bifurcation curves of limit cycles emanating from GH_1 and GH_2, respectively. The limit cycles emanating from the upper Hopf bifurcation branch are approaching the homoclinic cycle, however, the limit cycle curve with two saddle-nodes emanating from the Hopf bifurcation branch below will persist until the saddle-node point of limit cycle disappears. This has been illustrated in Figure 6A,B.

The whole bifurcation plane in Figure 6A, which is zoomed three times for clarity, shown in Figures 6B and Figure 7A,B, are divided into 12 regions. The corresponding phase portraits are given respectively in Figure 8. More specifically, we have region I: $a = 0.0458086, \beta = 1.49797$, a stable limit cycle contains an unstable hyperbolic positive equilibrium; II: $a = 0.0224992, \beta = 1.61114$, a big stable limit cycle contains a little unstable limit cycle enclosing a stable hyperbolic positive equilibrium, bistability states; III: $a = 0.0194589, \beta = 1.48903$, a stable hyperbolic

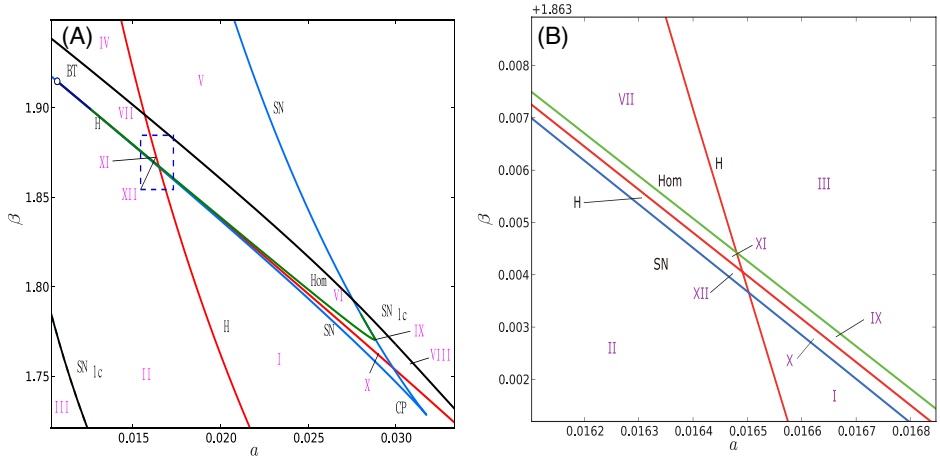

FIGURE 7 Zoomed two-parameter bifurcation diagram of system (7) where SN, H, Hom, SN_{lc} denote the saddle-node bifurcation curve (blue), Hopf bifurcation curve (red), homclinic bifurcation curve (green), and saddle-node curve (black) of limit cycles, respectively. (A) The second zoomed bifurcation diagram in Figure 6B for β vs. a. (B) The third zoomed bifurcation diagram in Figure 7A for β vs. a.

positive equilibrium; IV: $a = 0.0108446, \beta = 1.96406$, an unstable limit cycle contains a stable hyperbolic positive equilibrium, moreover, there exists a saddle point and a stable hyperbolic positive equilibrium, bistability states; V: $a = 0.0185468, \beta = 1.91789$, three hyperbolic positive equilibria (a saddle point, a stable focus, and an unstable focus) coexist; VI: $a = 0.0250827, \beta = 1.80629$, a stable limit cycle contains three hyperbolic positive equilibria (a saddle point, a stable focus, and an unstable focus), bistability states; VII: $a = 0.0147907, \beta = 1.89027$, a big stable limit cycle contains a little unstable limit cycle enclosing a stable hyperbolic positive equilibrium, moreover, there exists a saddle point and a stable hyperbolic positive equilibrium, tristability states; VIII: $a = 0.0312342, \beta = 1.74765$, a big stable limit cycle contains a little unstable limit cycle enclosing a stable hyperbolic positive equilibrium, bistability states; IX: $a = 0.0287306, \beta = 1.76738$, a big stable limit cycle contains a little unstable limit cycle enclosing a stable hyperbolic positive equilibrium, moreover, there exists a saddle point and an unstable hyperbolic positive equilibrium, bistability states; X: $a = 0.0301742, \beta = 1.74711$, a big stable limit cycle contains three hyperbolic positive equilibria (a saddle point, a stable focus, and two unstable focuses), bistability states; XI: $a = 0.0164697, \beta = 1.86736$, a big stable limit cycle contains a little unstable limit cycle enclosing a stable hyperbolic positive equilibrium, moreover, there exists a saddle point and a stable hyperbolic positive equilibrium, tristability states; XII: $a = 0.0164818, \beta = 1.86696$, a big stable limit cycle contains a little unstable limit cycle enclosing a stable hyperbolic positive equilibrium, moreover, there exists a saddle point and an unstable hyperbolic positive equilibrium, bistability states.

From the first generalized Hopf bifurcation point GH_1, the subcritical Hopf bifurcation point will be changed to the supercritical Hopf bifurcation point. There exists an interval for the parameter β between GH_1 and GH_2, where there is a saddle-node bifurcation point of limit cycle branch, that is, a stable limit cycle and an unstable limit cycle will coexist until they coalesce and persist. In particular, there is a whole saddle-node bifurcation curve of limit cycles rather than two distinct branches mentioned in Huang et al.[35] On the Hopf bifurcation curve, the left parts of GH_1

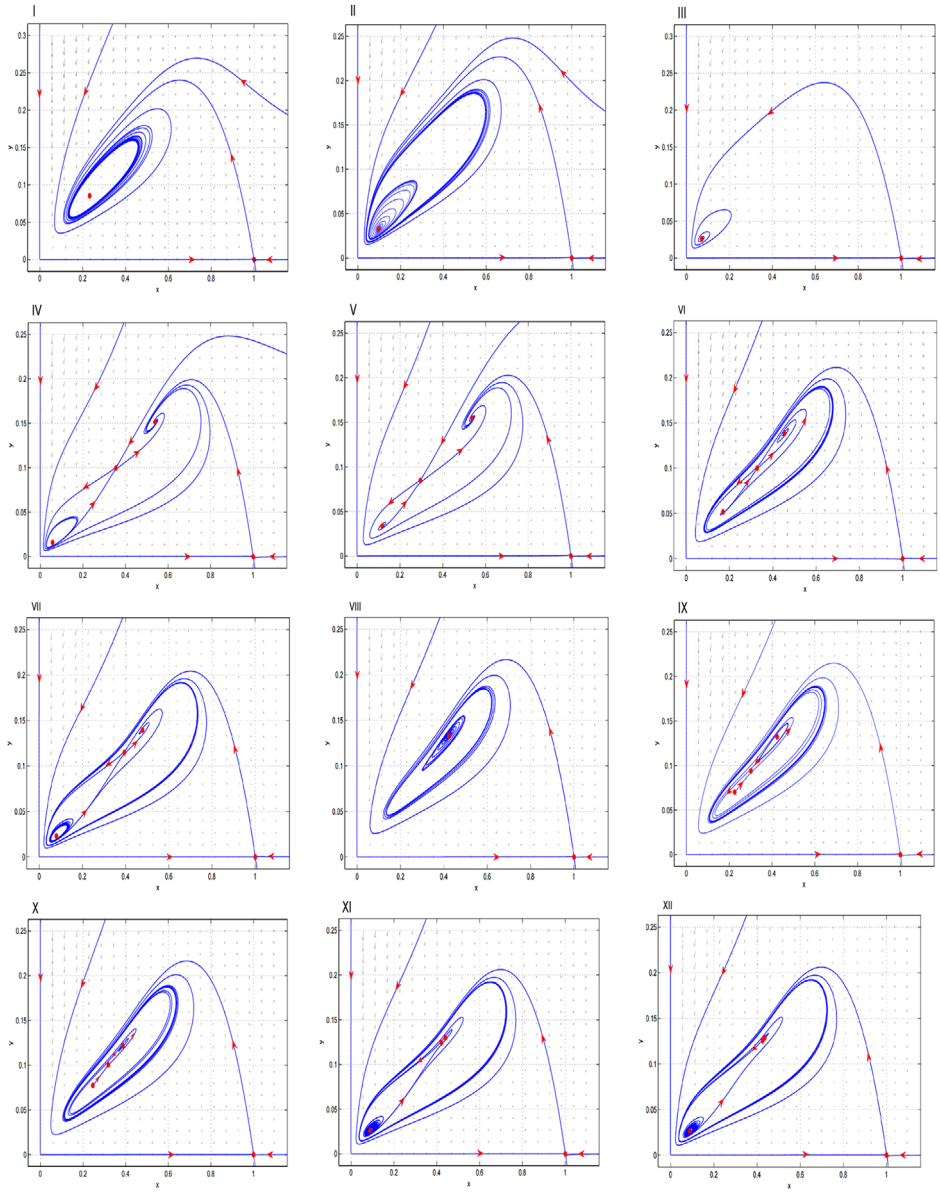

FIGURE 8 Phase portraits of regions I–XII shown in Figures 6 and 7.

and GH_2 are subcritical Hopf bifurcation curves and the right of them is a supercritical Hopf bifurcation curve, see Figure 6A,B.

4.3 | *d* as the primary bifurcation parameter

Setting d as the primary bifurcation parameter, we obtain the one-parameter bifurcation diagram. There are two subcritical Hopf bifurcation points $HB_1(1.19773 \times 10^{-1}, 3.45728 \times 10^{-2})$ as $d = 1.05728 \times 10^{-2}$ and $HB_2(4.34712 \times 10^{-1}, 1.25481 \times 10^{-1})$ as $d = 2.14803 \times 10^{-2}$. The first

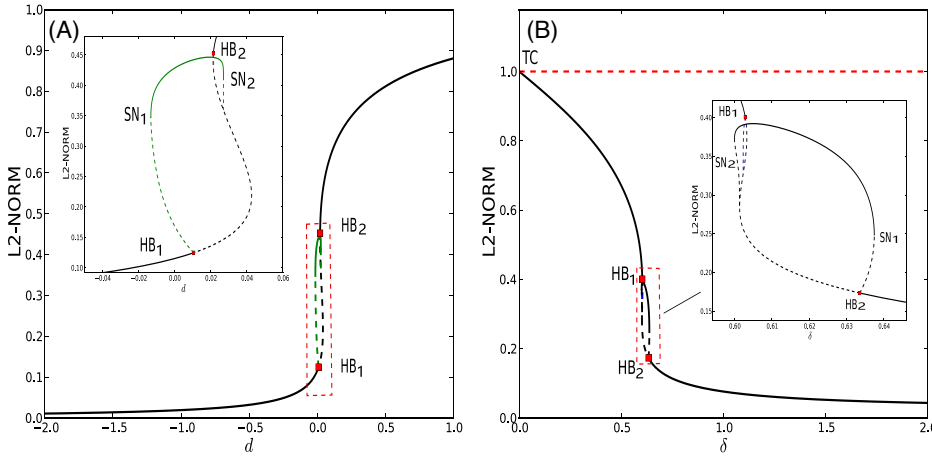

FIGURE 9 One-parameter bifurcation diagram of system (7). (A) L2-norm vs. d. (B) L2-norm vs. δ. Here, HB_1 and HB_2, SN_1 and SN_2, TC denote the Hopf bifurcation points and saddle-node bifurcation points of limit cycles, transcritical bifurcation point, respectively.

Lyapunov coefficients of HB_1 and HB_2 are, respectively, 1.540364×10^1 and 2.188749×10^1; two saddle-node bifurcation points $S\bar{N}_1(4.23305 \times 10^{-1}, 1.22188 \times 10^{-1})$ as $d = 2.13200 \times 10^{-2}$ and $S\bar{N}_2(2.09782 \times 10^{-1}, 6.05545 \times 10^{-2})$ as $d = 4.26926 \times 10^{-2}$. From the first Hopf bifurcation point HB_1, we have two saddle-node points of limit cycle $SN_1(5.10376 \times 10^{-1}, 1.41684 \times 10^{-1})$ as $d = -1.30903 \times 10^{-2}$, $period = 2.62507 \times 10^1$ and $SN_2(6.86965 \times 10^{-1}, 1.82966 \times 10^{-1})$ as $d = 2.70666 \times 10^{-2}$, $period = 6.10625 \times 10^1$ (see Figure 9A). Note that the metastability phenomenon is also found for the parameter d. In another word, the density of mite population will increase from the carrying capacity as d increases. Thus, the mite population may undergo outbreak.

Next, we set $a = 0.03, d = 0.05, \beta = 1.9107764064044153$ and take δ as the primary bifurcation parameter. We have two subcritical Hopf bifurcation points $HB_1(3.82285 \times 10^{-1}, 1.20613 \times 10^{-1})$ as $\delta = 6.02858 \times 10^{-1}$, $HB_2(1.64561 \times 10^{-1}, 5.45611 \times 10^{-2})$ as $\delta = 6.33529 \times 10^{-1}$, two saddle-node bifurcation points $S\bar{N}_1(3.57892 \times 10^{-1}, 1.12999 \times 10^{-1})$ as $\delta = 6.03299 \times 10^{-1}$ and $S\bar{N}_2(2.71488 \times 10^{-1}, 8.54400 \times 10^{-2})$ as $\delta = 6.01340 \times 10^{-1}$, one transcritical bifurcation point $TC(1, 0)$ as $\delta = 0$. The first Lyapunov coefficients of HB_1 and HB_2 are, respectively, 1.64117×10^1 and 5.289654×10^1; To continue from HB_2, we have two saddle-node points of limit cycles: $SN_1(3.30296 \times 10^{-1}, 1.07073 \times 10^{-1})$ as $\delta = 6.37431 \times 10^{-1}$, period $= 2.18099 \times 10^1$ and $SN_2(5.42326 \times 10^{-1}, 1.65980 \times 10^{-1})$ as $\delta = 5.99983 \times 10^{-1}$, period $= 5.45319 \times 10^1$. The limit cycles bifurcation form HB_1 and HB_2 are approaching distinct homoclinic cycles. Also note that the antimetastability is found for the parameter δ. Thus, the mite population may decrease as the parameter δ increases (Figure 9B).

4.4 | δ and d as the two primary bifurcation parameters

If we take δ and d as the two primary bifurcation parameters, then we have saddle-node bifurcation curve (blue), Hopf bifurcation curve (black), saddle-node bifurcation curve (red) of limit cycles. There are two cusp points $CP_1(3.10723 \times 10^{-1}, 1.01755 \times 10^{-1})$ as $\delta = 6.25735 \times 10^{-1}, d = 6.78302 \times 10^{-2}$, $CP_2(1.73206 \times 10^{-1}, 1.01407 \times 10^{-6})$ as $\delta = 1.11868 \times 10^{-5}$,

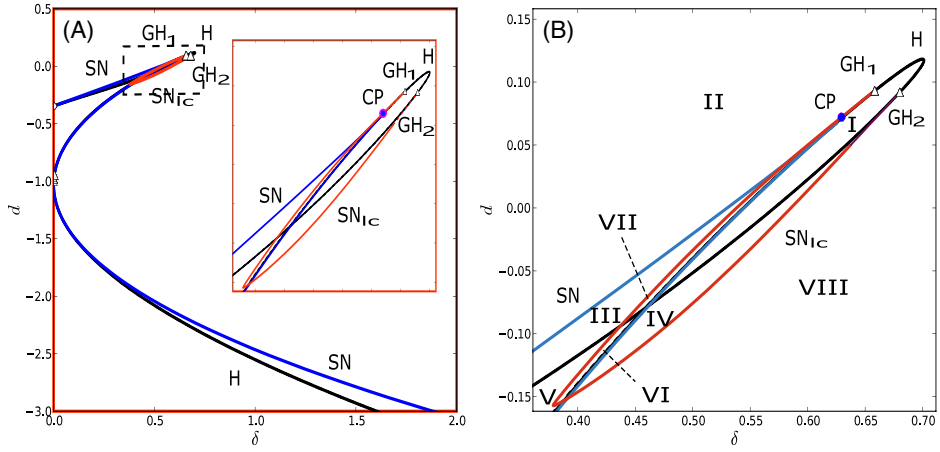

FIGURE 10 Two-parameter (δ vs. d) bifurcation diagram of system (7). (A) δ vs. d. (B) Zoomed bifurcation curve of δ vs. d with eight regions. Here, SN, H, SN_{lc} denote the saddle-node bifurcation curve (blue), Hopf bifurcation curve (black), saddle-node bifurcation curve of limit cycles (red).

$d = -3.46403 \times 10^{-1}$, two generalized Hopf bifurcation points $GH_1(3.24564 \times 10^{-1}, 1.11814 \times 10^{-1})$ as $\delta = 6.58274 \times 10^{-1}, d = 9.30543 \times 10^{-2}$, $GH_2(1.90789 \times 10^{-1}, 6.79109 \times 10^{-2})$ as $\delta = 6.80137 \times 10^{-1}, d = 9.18396 \times 10^{-2}$, one Bagdanov–Takens bifurcation point $BT(1.73183 \times 10^{-1}, 2.94846 \times 10^{-8})$ as $\delta = 3.25311 \times 10^{-7}, d = -3.46410 \times 10^{-1}$. The second Lyapunov coefficients of GH_1 and GH_2 are, respectively, -9.99813×10^2 and -7.502971×10^2; The saddle-node bifurcation curve of limit cycles is also connecting GH_1 and GH_2. This result is shown in Figure 10A,B.

The phase plane in Figure 10 is divided into eight regions and the corresponding phase portraits in those regions are shown in Figure 11. The following provides the details. I: $\delta = 0.648891, d = 0.0750986$, a stable limit cycle contains an unstable hyperbolic positive equilibrium; II: $\delta = 0.590287, d = 0.0848714$, a stable hyperbolic positive equilibrium; III: $\delta = 0.432085, d = -0.0791325$, three hyperbolic positive equilibria (a saddle point, a stable focus, and an unstable focus) coexist; IV: $\delta = 0.470348, d = -0.0853784$, a big stable limit cycle contains a little unstable limit cycle enclosing a stable hyperbolic positive equilibrium, bistability states; V: $\delta = 0.362312, d = -0.153302$, an unstable limit cycle contains a stable hyperbolic positive equilibrium, moreover, there exist a saddle point and a stable hyperbolic positive equilibrium, bistability states; VI: $\delta = 0.402356, d = -0.132842$, a big stable limit cycle contains a little unstable limit cycle enclosing a stable hyperbolic positive equilibrium, moreover, there exist a saddle point and a stable hyperbolic positive equilibrium, tristability states; VII: $\delta = 0.48071, d = -0.0542003$, a big stable limit cycle contains three hyperbolic positive equilibria (a saddle point, a stable focus, and an unstable focus), bistability states; VIII: $\delta = 0.598531, d = -0.0249369$, a stable hyperbolic positive equilibrium.

Combining the global bifurcation diagrams from Figure 6 to Figure 11, we can obtain the monostability, bistability, and tristability for equilibria and the number of limit cycle. These are summarized in Table 1.

Remark 2. Note that, here we find two generalized Hopf bifurcation points are connected by one saddle-node bifurcation curve of limit cycles, but it is different from that in Xu et al.,[52] where

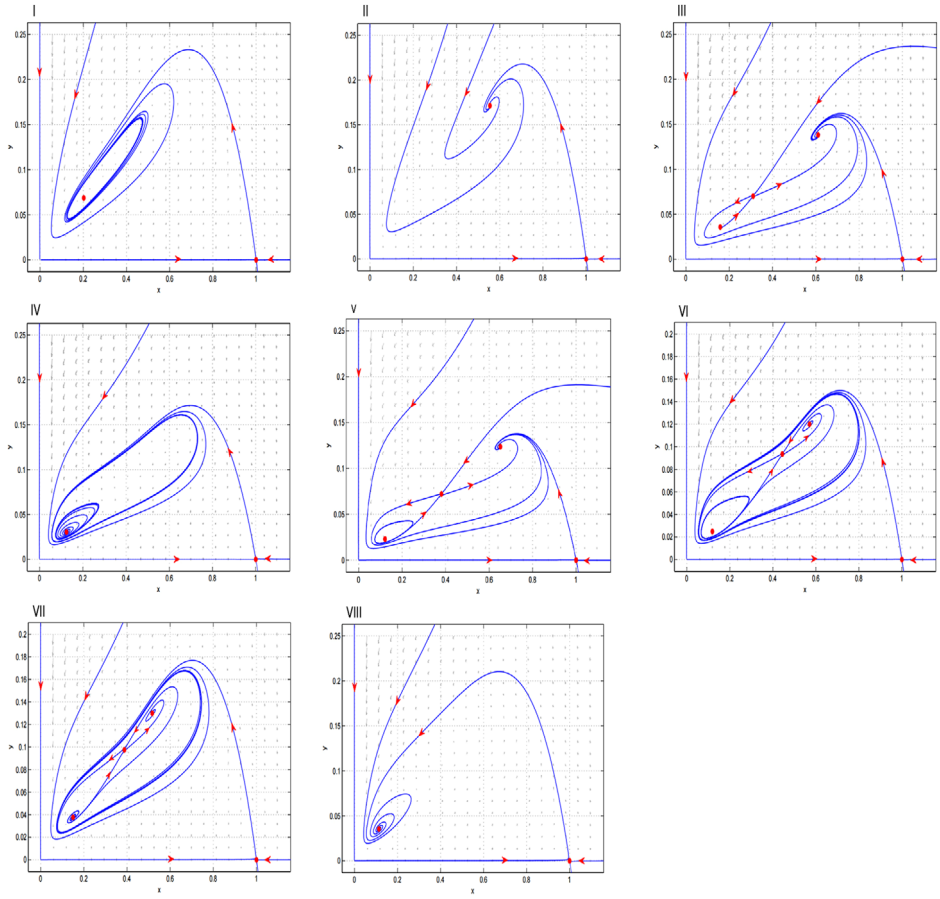

FIGURE 11 Phase portraits of regions I–VIII shown in Figure 10B.

TABLE 1 The classification of stability and the number of equilibria of system (7).

Stability	Equilibria	Regions
Monostability	Single equilibrium	Figure 8 III; Figure 11 II, VIII
	One equilibrium and one limit cycle	Figure 8I; Figure 11I
	Three equilibria	Figure 8V; Figure 11 III
	Three equilibria and one limit cycle	Figure 8X
Bistability	One equilibrium and two limit cycles	Figure 8 II, VIII; Figure 11 IV
	Three equilibria and one limit cycle	Figure 8 IV, VI; Figure 11V, VII
	Three equilibria and two limit cycles	Figure 8 IX, XII
Tristability	Three equilibria and two limit cycles	Figure 8 VII, XI; Figure 11 VI

the curve is on the top of Hopf bifurcation curve, so that the isola of limit cycles could be found. Further, it is also different from the scenario in Refs. [20, 32], where there exists a condimension 2 cusp of limit cycles indicating the coexistence of three limit cycles, which bifurcate from one Hopf bifurcation point.

Remark 3. Compared with the dynamics of Leslie type predator–prey system (1) with simplified Holling IV functional response (5) at $d = 0$ in Huang et al.,[35] in this paper we obtain some novel results for system (7) as follows:

(i) there are one or two Hopf bifurcation surfaces rather than only one;
(ii) there is one saddle-node loop bifurcation surface rather than only two;
(iii) there is one or two saddle-node bifurcation surface rather than only two.

Remark 4. As d increases, the whole bifurcation diagram of system (7) including the location of the intersection point of Hopf bifurcation curve, Hopf bifurcation curve, homoclinic bifurcation curve, and saddle-node bifurcation curve, bifurcation point will be moved to the left bottom of the plane.

5 | CONCLUSION AND DISCUSSION

In this paper, we conducted a detailed bifurcation analysis of a predator–prey mite model with generalized Holling Type IV functional response, which can be used to describe the interaction between the predator *M. occidentalis* and the prey phytophagous spider mite Tetranychus mcdanieli on fruit trees. The euryphagous nature is crucial for the predator to survive in nature. It has a common characteristic of species, leading to the coexistence of two species. The simple model was shown to exhibit very complex dynamics. By using the bifurcation analysis, we have found that there are up to three equilibrium states (see Table 1). All the possible scenarios of the associated bifurcation and dynamical behaviors are investigated.

Collings[28] studied a predator–prey mite model of Leslie type with Holling Type IV function and considered the role of temperature in the growth of mites. On top of the existence of a stable low population density equilibrium, population cycles or population outbreaks in response to perturbations were shown with different sets of parameter values. Li and Xiao[33] investigated the model (7) with $d = 0$, showing the existence of codimension 2 cusp bifurcation and codimension 2 Bagdanov–Takens bifurcation without considering codimension 3 cusp bifurcation. Huang et al.[35] showed that for the model (7) with $d = 0$ and a simplified Holling Type IV functional response, there exists a degenerate Bogdanov–Takens singularity (focus type) of codimension 3 for some parameter values. Bistability (one stable equilibrium and one stable limit cycles) and tristability (two stable equilibria and one stable limit cycle) can emerge with certain parameter values. In this paper, the predator–prey mite model (7) with a generalized Holling type IV functional response is investigated in details using dynamical system approach. We found a degenerate Bogdanov–Takens singularity (focus type) of codimension 3 and a degenerate Bogdanov–Takens singularity (cusp type) of codimension 3 for some parameter values. Meanwhile, the complete bifurcation diagrams and their dynamics are studied analytically and illustrated numerically.

Of note, we find that there exist one or two Hopf bifurcation curves, one saddle node bifurcation curve of limit cycle, one or two saddle-node bifurcation curves for model (7). Therefore, model (7) may have three hyperbolic positive equilibria, two limit cycles, bistability (one stable equilibrium and one stable limit cycle, or two stable equilibria), or tristability (two stable equilibria and one stable limit cycles). Huang et al.[35] did not present the whole bifurcation diagram, and mentioned that there are one Hopf bifurcation curve, two saddle node bifurcation curve of limit cycles. Actually, the saddle node bifurcation curve of limit cycles is connecting with two generalized Hopf bifurcation points. We evaluated the role of parameter d, which describes the effect

of "inhibition" in microbial dynamics and "group defense" in population dynamics as Freedman and Wolkowicz[27] mentioned. We find that it does not change the bifurcation structure but moves the location of bifurcation diagram to the left bottom as the parameter d increases.

Different phase portraits of model (7) are obtained by numerical simulations. We showed that model (7) can have: (i) a stable limit cycle contains an unstable hyperbolic positive equilibrium (monostability); (ii) a stable limit cycle enclosing three positive equilibria and a homoclinic cycle (bistability); (iii) a big limit cycle containing a small limit cycle and three hyperbolic positive equilibria (tristability), and so forth. Therefore, our results provide the whole bifurcation dynamics of model (7) both analytically and numerically. In addition, we found that the most significant consequence of the metastability and hysteresis exhibited by system (7) is that these results can be used to describe the outbreaks of mites.

We conclude this study by noting that the dynamics of this generalist predator–prey mite model are very rich. Three parameters are used to analyze the dynamical behavior. The codimension 3 Bagdanov–Taken bifurcation serves as an organizing center for the complex dynamics of the mite model. Furthermore, it will be very interesting to study the existence of isola bifurcation of limit cycles in Xu et al.[52,53] It exists for model (7) if the generalized Holling IV functional response (5) is replaced by Holling II functional response (3) and the intrinsic rates of mites are replaced by the functions depending on temperature mentioned in Collings and Wollkind.[54] This is left for future investigation.

ACKNOWLEDGMENTS

L. Rong is supported by the National Science Foundation grants DMS-2324692 and DMS-1950254.

DATA AVAILABILITY STATEMENT

Data sharing not applicable to this article as no data sets were generated or analyzed during the current study.

ORCID

Libin Rong https://orcid.org/0000-0002-1464-6078

REFERENCES

1. Wollkind DJ, Logan JA. Temperature-dependent predator-prey mite ecosystem on apple tree foliage. *J Math Biol*. 1978;6:265-283. doi:10.1007/BF02547801
2. Zehnder G, Gurr GM, Kühne S, Wade MR, Wratten SD, Wyss E. Arthropod pest management in organic crops. *Annu Rev Entomol*. 2007;52:57-80. doi:10.1146/annurev.ento.52.110405.091337
3. Croft BA, Macrae IV. Biological control of apple mites by mixed populations of *Metaseiulus occidentalis* (Nesbitt) and *Typhlodromus pyri* Scheuten (Acari: Phytoseiidae). *Environ Entomol*. 1992;21:202-209. doi:10.1093/ee/21.1.202
4. Croft BA, MacRae IV, Currans KG. Factors affecting biological control of apple mites by mixed populations of *Metaseiulus occidentalis* and *Typhlodromus pyri*. *Exp Appl Acarol*. 1992;14:343-355. doi:10.1007/BF01200572
5. Cuthbertson AG, Murchie AK. The phenology, oviposition and feeding rate of Anystis baccarum, a predatory mite in Bramley apple orchards in Northern Ireland. *Exp Appl Acarol*. 2004;34:367-373. doi:10.1023/B:APPA.0000049218.61282.d1
6. Hoyt SC. Population studies of five mite species on apple in Washington. In: Proceedings, 2nd International Congress Acarology. Sutton-Bonnington, England. Acad Kiado, Budapest. 1969:117-133.
7. Zhang ZF, Ding TR, Huang WZ, Dong ZX. *Qualitative Theory of Differential Equations*. American Mathematical Society; 2006:101.

8. Ye GY, Xiao Q, Chen M, et al. Tea: biological control of insect and mite pests in China. *Biol Control*. 2014;68:73-91. doi:10.1016/j.biocontrol.2013.06.013
9. Schmidt T. *Apple Pesticide Residue Study Report*. Washington Tree Fruit Research Commission; 2021.
10. A new report: Biological pest control market research report: Biological pest control market size by application (vegetables, turf and gardening, crop, fruit, other, building), by type (predatory mites, insects, nematodes, other), by region (North America, Europe, Asia-Pacific, rest of the world), market analysis report, forecast 2021-2026. *Mark Res Eng*. 2021:1-146.
11. May RM. *Complexity and Stability in Model Ecosystems*. Princeton University Press; 1973.
12. Wollkind DJ, Collings JB, Logan JA. Metastability in a temperature-dependent model system for predator-prey mite outbreak interactions on fruit trees. *Bull Math Biol*. 1988;50:379-409. doi:10.1016/S0092-8240(88)90005-5
13. Leslie PH. Some further notes on the use of matrices in population mathematics. *Biometrika*. 1948;35:213-245. doi:10.2307/233234
14. Hsu SB, Huang TW. Global stability for a class of predator-prey systems. *SIAM J Appl Math*. 1995;55:763-783. doi:10.1137/S0036139993253201
15. Korobeinikov A. A Lyapunov function for Leslie-Gower predator-prey models. *Appl Math Lett*. 2001;14:697-699. doi:10.1016/S0893-9659(01)80029-X
16. Cheng KS. Uniqueness of a limit cycle for a predator-prey system. *SIAM J Math Anal*. 1981;12:541-548. doi:10.1137/0512047
17. Gasull A, Kooij RE, Torregrosa J. Limit cycles in the Holling-Tanner model. *Publ Mat*. 1997;41:149-167. doi:10.5565/PUBLMAT_41197_09
18. Sáez E, González-Olivares E. Dynamics of a predator-prey model. *SIAM J Appl Math*. 1999;59:1867-1878. doi:10.1137/S0036139997318457
19. Lan KQ, Zhu CR. Phase portraits, Hopf bifurcations and limit cycles of the Holling-Tanner models for predator-prey interactions. *Nonlinear Anal RWA*. 2011;12:1961-1973. doi:10.1016/j.nonrwa.2010.12.012
20. Xu YC, Yang Y, Meng FW, Ruan SG. Degenerate codimension-2 cusp of limit cycles in a Holling-Tanner model with harvesting and anti-predator behavior. *Nonlinear Anal RWA*. 2024;76:103995. doi:10.1016/j.nonrwa.2023.103995
21. Holling CS. The functional response of predators to prey density and its role in mimicry and population regulation. *Memoirs Entomol Soc Can*. 1965;97:5-60. doi:10.4039/entm9745fv
22. Xiao DM, Ruan SG. Global analysis in a predator-prey system with nonmonotonic functional response. *SIAM J Appl Math*. 2001;61:1445-1472. doi:10.1137/S0036139999361896
23. Jost J, Drake J, Fredrickson A, Tsuchiya H. Interactions of *Tetrahymena Pyriformis*, *Escherichia coli*, *Azotobacter vinelandii*, and glucose in a minimal medium. *J Bacteriol*. 1973;113:834-840. doi:10.1128/jb.113.2.834-840.1973
24. Jost J, Drake J, Tsuchiya H, Fredrickson A. Microbial food chains and food webs. *J Theor Biol*. 1973;41:461-484. doi:10.1016/0022-5193(73)90056-8
25. Huang JC, Ruan SG, Song J. Bifurcations in a predator-prey system of leslie type with generalized Holling type III functional response. *J Differ Equ*. 2014;257:1721-1752. doi:10.1016/j.jde.2014.04.024
26. Lin XQ, Xu YC, Gao DZ, Fan GH. Bifurcation and overexploitation in Rosenzweig-Macarthur model. *Discrete & Cont Dynam Syst Ser B*. 2022;28:690-706. doi:10.3934/dcdsb.2022094
27. Freedman HI, Wolkowicz GS. Predator-prey systems with group defence: the paradox of enrichment revisited. *Bull Math Biol*. 1986;48:493-508. doi:10.1016/S0092-8240(86)90004-2
28. Collings JB. The effects of the functional response on the bifurcation behavior of a mite predator-prey interaction model. *J Math Biol*. 1997;36:149-168. doi:10.1007/s002850050095
29. Andrews JF. A mathematical model for the continuous culture of microorganisms utilizing inhibitory substrates. *Biotechnol Bioengin*. 1968;10:707-723. doi:10.1002/bit.260100602
30. Atabaigi A, Barati A. Relaxation oscillations and canard explosion in a predator-prey system of Holling and Leslie types. *Nonlinear Anal RWA*. 2017;36:139-153. doi:10.1016/j.nonrwa.2017.01.006
31. Wolkowicz GSK. Bifurcation analysis of a predator-prey system involving group defence. *SIAM J Appl Math*. 1988;48:592-606. doi:10.1137/0148033
32. Wen T, Xu YC, He M, Rong LB. Modelling the dynamics in a predator-prey system with Allee effects and anti-predator behavior. *Qual Theor Dyn Syst*. 2023;2023:1-50. doi:10.1007/s12346-023-00821-z

33. Li YL, Xiao DM. Bifurcations of a predator-prey system of Holling and Leslie types. *Chaos, Solitons Fractals*. 2007;34:606-620. doi:10.1016/j.chaos.2006.03.068
34. Broer HW, Naudot V, Roussarie R, Saleh K. Bifurcations of a predator-prey model with non-monotonic response function. *Compt Rend Math*. 2005;341:601-604. doi:10.1016/j.crma.2005.09.033
35. Huang JC, Xia XJ, Zhang XA, Ruan SG. Bifurcation of codimension 3 in a predator-prey system of Leslie type with simplified Holling type IV functional response. *Inter J Bifur & Chaos*. 2016;26:1650034. doi:10.1142/S0218127416500346
36. Dai YF, Zhao YL. Hopf cyclicity and global dynamics for a predator-prey system of Leslie type with simplified Holling type IV functional response. *Inter J Bifur & Chaos*. 2018;28:1850166. doi:10.1142/S0218127418501663
37. Zhang J, Su J. Bifurcations in a predator-prey model of Leslie-type with simplified Holling type IV functional response. *Inter J Bifur & Chaos*. 2021;31:2150054. doi:10.1142/S0218127421500541
38. Xiao DM, Zhu HP. Multiple focus and hopf bifurcations in a predator-prey system with nonmonotonic functional response. *SIAM J Appl Math*. 2006;66:802-819. doi:10.1137/050623449
39. Rothe F, Shafer DS. Multiple bifurcation in a predator-prey system with nonmonotonic predator response. *Proc R Soc Edinburgh Sect A: Math*. 1992;120:313-347. doi:10.1017/S0308210500032169
40. Lawrence P. *Differential Equations and Dynamical Systems*. Springer; 2001.
41. Huang JC, Gong YJ, Ruan SG. Bifurcation analysis in a predator-prey model with constant-yield predator harvesting. *Discrete & Contin Dyn Syst, Ser B*. 2013;18:2101-2121. doi:10.3934/dcdsb.2013.18.2101
42. Lamontagne Y, Coutu C, Rousseau C. Bifurcation analysis of a predator-prey system with generalised Holling type III functional response. *J Dyn Differ Equ*. 2008;20:535-571.
43. Cai LL, Chen GT, Xiao DM. Multiparametric bifurcations of an epidemiological model with strong Allee effect. *J Math Biol*. 2013;67:185-215. doi:10.1007/s0085-01-0546-5
44. Bogdanov RI. Bifurcation of the limit cycle of a family of plane vector field. *Sel Math Sov*. 1981;4:373-387.
45. Takens F. *Forced Oscillations and Bifurcations*. Springer; 1974.
46. Li CZ, Li JQ, Ma ZE. Codimension 3 BT bifurcations in an epidemic model with a nonlinear incidence. *Discrete & Contin Dynam Syst Ser B*. 2015;20:1107-1116. doi:10.3934/dcdsb.2015.20.1107
47. Dumortier F, Roussarie R, Sotomayor J. Generic 3-parameter families of vector fields on the plane, unfolding a singularity with nilpotent linear part. The cusp case of codimension 3. *Ergodic Theory & Dynam Systems*. 1987;7:375-413. doi:10.1017/S0143385700004119
48. Chow SN, Li CZ, Wang D. *Normal Forms and Bifurcation of Planar Vector Fields*. Cambridge University Press; 1994.
49. Yu P, Zhang WJ. Complex dynamics in a unified SIR and HIV disease model: a bifurcation theory approach. *J Nonlinear Sci*. 2019;29:2447-2500. doi:10.1007/s00332-019-09550-7
50. Xiao DM, Zhang K. Multiple bifurcations of a predator-prey system. *Discrete & Contin Dynam Syst Ser B*. 2012;8:417-433. doi:10.3934/dcdsb.2007.8.417
51. Doedel EJ, Oldeman BE. AUTO-07P: Continuation and bifurcation software for ordinary differential equations. Technical Report, Concordia University, 2009.
52. Xu YC, Zhu ZR, Yang Y, Meng FW. Vectored immunoprophylaxis and cell-to-cell transmission in HIV dynamics. *Inter J Bifur & Chaos*. 2020;30:2050185. doi:10.1142/S0218127420501850
53. Sandstede B, Xu YC. Snakes and isolas in non-reversible conservative systems. *Dynam Syst*. 2012;27:317-329. doi:10.1080/14689367.2012.691961
54. Collings JB, Wollkind DJ. A global analysis of a temperature-dependent model system for a mite predator-prey interaction. *SIAM J Appl Math*. 1990;50:1348-1372. doi:10.1137/0150081

How to cite this article: Yang Y, Xu Y, Rong L, Ruan S. Bifurcations and global dynamics of a predator–prey mite model of Leslie type. *Stud Appl Math*. 2024;152:1251–1304. https://doi.org/10.1111/sapm.12675

APPENDIX: REPRESENTATION OF σ_{22}

$$\sigma_{22} = -(t_0 + t_1 m + t_2 m^2 + t_3 m^3 + t_4 m^4 + t_5 m^5 + t_6 m^6 + t_7 m^7 + t_8 m^8 + t_9 m^9),$$

where

$$\begin{aligned}
t_0 = {} & a^7(-5d - 10) + a^6\left(-157d^3 - 1265d^2 - 3335d - 2864\right) + a^5(-1278d^4 - 11564d^3 - \\
& 38326d^2 - 54535d - 27802) + a^4(-3419d^5 - 33643d^4 - 127899d^3 - 231257d^2 - \\
& 194202d - 57858) + a^3(-1265d^6 - 5682d^5 + 23626d^4 + 212261d^3 + 553903d^2 + \\
& 635839d + 275634) + a^2(9922d^7 + 149699d^6 + 951992d^5 + 3313998d^4 + 6829825d^3 \\
& + 8341406d^2 + 5593467d + 1588596) + a(17424d^8 + 272297d^7 + 1843401d^6 + \\
& 7060798d^5 + 16733611d^4 + 25117387d^3 + 23302731d^2 + 12201261d + 2754450) + \\
& 8976d^9 + 150206d^8 + 1107969d^7 + 4723857d^6 + 12813377d^5 + 22894374d^4 + \\
& 26886435d^3 + 19948008d^2 + 8444646d + 1542942,
\end{aligned}$$

$$\begin{aligned}
t_1 = {} & a^8(5d + 5) + a^7\left(-163d^2 - 929d - 1366\right) + a^6(-964d^3 - 4609d^2 - 5319d + 996) + a^5 \\
& \times(2235d^4 + 34341d^3 + 155267d^2 + 275610d + 167759) + a^4(26246d^5 + 298379 \\
& \times d^4 + 1297651d^3 + 2698434d^2 + 2676907d + 1007837) + a^3(65618d^6 + 761821d^5 + \\
& 3561642d^4 + 8532773d^3 + 10944995d^2 + 7011741d + 1696452) + a^2(54784d^7 + 608890 \\
& \times d^6 + 2655113d^5 + 5461934d^4 + 4228003d^3 - 2632009d^2 - 6534035d - 3095898) + a \\
& \times(-12426d^8 - 338465d^7 - 3224458d^6 - 15780023d^5 - 45232886d^4 - 79289920d^3 - \\
& 83862671d^2 - 49204734d - 12293373) - 28776d^9 - 531685d^8 - 4281537d^7 - 19749174 \\
& \times d^6 - 57535282d^5 - 109764684d^4 - 136988820d^3 - 107619372d^2 - 48118590d - \\
& 9274860,
\end{aligned}$$

$$\begin{aligned}
t_2 = {} & 5a^9 + a^8(-65d - 83) + a^7\left(-25d^2 + 2599d + 6362\right) + a^6(6117d^3 + 49093d^2 + 115235 \\
& \times d + 75673) + a^5(31391d^4 + 231968d^3 + 572089d^2 + 511616d + 101938) + a^4(43919 \\
& \times d^5 + 232110d^4 + 55923d^3 - 1560052d^2 - 2992165d - 1611895) + a^3(-44294d^6 - \\
& 907971d^5 - 6036748d^4 - 18819793d^3 - 30233192d^2 - 24137815d - 7535086) + a^2 \\
& \times(-146861d^7 - 2135708d^6 - 12542249d^5 - 38629876d^4 - 67060115d^3 - 64644386d^2 \\
& -30888125d - 5070033) + a(-63507d^8 - 741436d^7 - 3013448d^6 - 2829990d^5 + \\
& 16117128d^4 + 61445629d^3 + 94230012d^2 + 70252528d + 20938509) + 36336d^9 + \\
& 774836d^8 + 7026651d^7 + 35868254d^6 + 114168041d^5 + 235710477d^4 + 316115759d^3 \\
& + 265547469d^2 + 126580320d + 25992690,
\end{aligned}$$

$$t_3 = -61a^9 + a^8(-243d - 306) + a^7\left(1781d^2 + 3386d - 4662\right) + a^6(8287d^3 + 2470d^2 - 92792d - 103513) + a^5(-13969d^4 - 262478d^3 - 1077609d^2 - 1518843d - 657396) + a^4(-109360d^5 - 1131354d^4 - 4079215d^3 - 6300683d^2 - 3902017d - 587817) + a^3 \times (-126931d^6 - 960784d^5 - 1533008d^4 + 4733740d^3 + 19000615d^2 + 22793878d + 9352650) + a^2(66842d^7 + 1689136d^6 + 13851870d^5 + 54884543d^4 + 118877653d^3 + 143563104d^2 + 90180588d + 22686513) + a(119238d^8 + 1965982d^7 + 13127393d^6 + 46147265d^5 + 91422061d^4 + 98155724d^3 + 43535897d^2 - 8169045d - 10313571) - 22512d^9 - 593276d^8 - 6322932d^7 - 36769918d^6 - 130578395d^5 - 296411157d^4 - 432562927d^3 - 392598951d^2 - 201338112d - 44419005,$$

$$t_4 = 158a^9 + a^8(1724d + 2804) + a^7\left(4965d^2 + 14268d + 16362\right) + a^6(-5584d^3 - 25656d^2 + 18358d + 54699) + a^5(-36863d^4 - 124717d^3 + 178037d^2 + 753221d + 474072) + a^4 \times (14430d^5 + 586443d^4 + 3595825d^3 + 8241624d^2 + 8003120d + 2793603) + a^3(157524d^6 + 2003302d^5 + 9117448d^4 + 18733077d^3 + 16811688d^2 + 3611916d - 1971590) + a^2 \times (80000d^7 + 433095d^6 - 2291296d^5 - 24245227d^4 - 78456218d^3 - 122912365d^2 - 95103888d - 29087351) + a(-83964d^8 - 1838277d^7 - 15538928d^6 - 68557689d^5 - 175407670d^4 - 267888188d^3 - 237486390d^2 - 109711261d - 19220730) + 6816d^9 + 247960d^8 + 3313101d^7 + 22885745d^6 + 93315421d^5 + 237732461d^4 + 383278157d^3 + 380181825d^2 + 211611134d + 50495349,$$

$$t_5 = -104a^9 + a^8(-1529d - 2987) + a^7\left(-8316d^2 - 28863d - 28914\right) + a^6(-14901d^3 - 66136d^2 - 130599d - 91631) + a^5(18270d^4 + 137059d^3 + 208384d^2 + 16201d - 50887) + a^4(62130d^5 + 333568d^4 + 10314d^3 - 2150665d^2 - 3592848d - 1786848) + a^3(-29434 \times d^6 - 880515d^5 - 6297726d^4 - 19003755d^3 - 27807472d^2 - 19246903d - 4858452) + a^2 \times (-93268d^7 - 1349742d^6 - 6826211d^5 - 14381383d^4 - 6885800d^3 + 20351230d^2 + 32152131d + 13922929) + a(26778d^8 + 871117d^7 + 9477090d^6 + 50820716d^5 + 154158001d^4 + 277544238d^3 + 293503352d^2 + 167751957d + 39701973) - 804d^9 - 51461d^8 - 980091d^7 - 8638694d^6 - 42237563d^5 - 124187554d^4 - 225362939d^3 - 247429065d^2 - 150756139d - 39116631,$$

$$t_6 = 43a^9 + a^8(531d + 1125) + a^7\left(3471d^2 + 14053d + 16282\right) + a^6(12889d^3 + 76385d^2 + 161345d + 112616) + a^5(12519d^4 + 91188d^3 + 289149d^2 + 380297d + 145624) + a^4$$

$$\times(-30573d^5 - 283124d^4 - 806101d^3 - 898130d^2 - 283938d + 112078) + a^3(-32832d^6 - 169081d^5 + 512108d^4 + 4511927d^3 + 10146086d^2 + 9690277d + 3399598) + a^2(34179 \times d^7 + 799974d^6 + 6125073d^5 + 22121447d^4 + 42433723d^3 + 43652232d^2 + 21804947d + 3709672) + a(-3219d^8 - 208464d^7 - 3156026d^6 - 21121157d^5 - 76014844d^4 - 158206991d^3 - 191043974d^2 - 124380259d - 33763131) + 3744d^8 + 147063d^7 + 1891684d^6 + 11836146d^5 + 41648252d^4 + 86951029d^3 + 107114829d^2 + 72042443d + 20419917,$$

$$t_7 = -5a^9 + a^8(-109d - 262) + a^7\left(-473d^2 - 2134d - 3062\right) + a^6(-2659d^3 - 21206d^2 - 55636d - 46416) + a^5(-9175d^4 - 97742d^3 - 346651d^2 - 488216d - 225548) + a^4 \times(-1544d^5 - 19670d^4 - 94613d^3 - 150483d^2 - 46032d + 21556) + a^3(16915d^6 + 232156d^5 + 1083908d^4 + 2450992d^3 + 2901613d^2 + 1683480d + 365882) + a^2(-4302d^7 - 206812d^6 - 2237626d^5 - 10506592d^4 - 25906733d^3 - 35210044d^2 - 25027570d - 7280260) + a(19838d^7 + 526767d^6 + 4768214d^5 + 21051615d^4 + 51263124d^3 + 70600139d^2 + 51694486d + 15679533) - 8928d^7 - 218570d^6 - 1928652d^5 - 8511446d^4 - 20977649d^3 - 29439519d^2 - 22055549d - 6863802,$$

$$t_8 = a^8(10d + 28) + a^7\left(61d^2 + 245d + 340\right) + a^6(-9d^3 - 93d^2 + 1621d + 3472) + a^5(1387d^4 + 19917d^3 + 86947d^2 + 144225d + 77844) + a^4(3139d^5 + 48554d^4 + 245820d^3 + 534299 \times d^2 + 518329d + 188176) + a^3(-2277d^6 - 59664d^5 - 435482d^4 - 1513592d^3 - 2771469 \times d^2 - 2570545d - 956756) + a^2(20540d^6 + 356968d^5 + 2182070d^4 + 6585745d^3 + 10689649d^2 + 8977655d + 3076016) + a(-32719d^6 - 506090d^5 - 2957605d^4 - 8707405d^3 - 13884131d^2 - 11492197d - 3886164) + 9840d^6 + 155295d^5 + 932956d^4 + 2820084d^3 + 4602657d^2 + 3887665d + 1337940,$$

$$t_9 = a^7\left(-5d^2 - 28d - 36\right) + a^6\left(5d^3 + 89d^2 + 194d - 8\right) + a^5(19d^4 + 172d^3 - 71d^2 - 1432 \times d - 1068) + a^4(-432d^5 - 8583d^4 - 52345d^3 - 137727d^2 - 164474d - 74296) + a^3 \times(4562d^5 + 49592d^4 + 222850d^3 + 498593d^2 + 546276d + 234692) + a^2(-16418d^5 - 155554d^4 - 600723d^3 - 1171601d^2 - 1146098d - 448888) + a(16100d^5 + 153269d^4 + 584546d^3 + 1114107d^2 + 1059856d + 402828) - 3852d^5 - 39143d^4 - 156105d^3 - 306585d^2 - 297494d - 114504.$$